

Certified Reduced Basis Methods for Parametrized Distributed Optimal Control Problems

Mark Kärcher · Martin A. Grepl · Karen Veroy

Received: date / Accepted: date

Abstract In this paper, we consider the efficient and reliable solution of distributed optimal control problems governed by parametrized elliptic partial differential equations. The reduced basis method is used as a low-dimensional surrogate model to solve the optimal control problem. To this end, we introduce reduced basis spaces not only for the state and adjoint variable but also for the distributed control variable. We also propose two different error estimation procedures that provide rigorous bounds for the error in the optimal control and the associated cost functional. The reduced basis optimal control problem and associated *a posteriori* error bounds can be efficiently evaluated in an offline-online computational procedure, thus making our approach relevant in the many-query or real-time context. We compare our bounds with a previously proposed bound based on the Banach-Nečas-Babuška (BNB) theory and present numerical results for two model problems: a Graetz flow problem and a heat transfer problem.

Keywords Optimal control · reduced basis method · a posteriori error estimation · model order reduction · parameter-dependent systems · partial differential equations · elliptic problems

Mathematics Subject Classification (2000) 49J20 · 65K10 · 65M15 · 65M60 · 93C20

This work was supported by the Excellence Initiative of the German federal and state governments and the German Research Foundation through Grant GSC 111.

Mark Kärcher
Aachen Institute for Advanced Study in Computational Engineering Science (AICES), RWTH Aachen University, Schinkelstraße 2, 52062 Aachen, Germany
E-mail: kaercher@aices.rwth-aachen.de

Martin A. Grepl
Numerical Mathematics, RWTH Aachen University, Templergraben 55, 52056 Aachen, Germany
E-mail: grepl@igpm-rwth-aachen.de

Karen Veroy
Aachen Institute for Advanced Study in Computational Engineering Science (AICES), RWTH Aachen University, Schinkelstraße 2, 52062 Aachen, Germany
E-mail: veroy@aices.rwth-aachen.de

1 Introduction

Many problems in science and engineering can be modeled in terms of optimal control problems governed by parametrized partial differential equations (PDEs), see e.g. [25, 13, 24, 34] for theoretical results and applications. While the PDE describes the underlying system or component behavior, the parameters often serve to identify a particular configuration of the component — such as boundary and initial conditions, material properties, and geometry. In such cases — in addition to solving the optimal control problem itself — one is often interested in exploring many different parameter configurations and thus in speeding up the solution of the optimal control problem. However, using classical discretization techniques such as finite elements or finite volumes even a single solution is often computationally expensive and time-consuming, a parameter-space exploration thus prohibitive. One way to decrease the computational burden is the surrogate model approach, where the original high-dimensional model is replaced by a reduced order approximation. These ideas have received a lot of attention in the past and various model order reduction techniques have been used in this context: proper orthogonal decomposition (POD) e.g. in [22, 2, 23, 35], reduction based on inertial manifolds in [15], and reduced basis methods in [16, 7, 21, 20, 29]. However, the solution of the reduced order optimal control problem is generally suboptimal and reliable error estimation is thus crucial.

In this paper we employ the reduced basis method [30, 32] as a surrogate model for the solution of *distributed* optimal control problems governed by parametrized elliptic partial differential equations. We extend our previous work in [11, 21, 20] in several directions. First, we consider optimal control problems involving distributed controls. Distributed controls pose an additional challenge relative to scalar controls since the control space is also high-dimensional. To this end, we follow the approach originally proposed in [18] and introduce reduced basis spaces not only for the state and adjoint variable but also a separate reduced basis (control) space for the distributed control. We thus obtain a considerable dimension reduction of the first-order optimality system. Second, we propose two new *a posteriori* error bounds for the optimal control and associated cost functional. The first proposed bound is an extension of our work in [11, 21] to distributed controls, the second bound is derived directly from the error residual equations of the optimality system. Third, we compare our proposed bounds to the bound recently proposed in [29]. Finally, we show that the reduced order optimal control problem *and* error bounds can be efficiently evaluated in an offline-online computational procedure.

A posteriori error bounds for reduced order solutions of optimal control problems have been proposed for proper orthogonal decomposition (POD) and reduced basis surrogate models in [35] and [7, 29], respectively. In [35], the authors estimate the distance between the computed suboptimal control and the unknown optimal control using a perturbation argument proposed in [12, 26]. The approach allows one to use the POD approximation to efficiently solve the optimal control problem. The evaluation of the *a posteriori* error bounds, however, requires a “forward-backward” solution of the underlying high-dimensional state and adjoint equations and, as pointed out in [35], is thus computationally expensive. Furthermore, in the case of distributed controls there is no reduction of the possibly high-dimensional control space.

In [29], a reduced basis approach to distributed optimal control problems has been considered. The resulting *a posteriori* error bound follows directly from previous work on reduced basis methods for noncoercive problems [36]. However, the development in [36] only provides a combined bound for the error in the state, adjoint, and control variables. Furthermore, the approach requires the computation of (a lower bound to) the parameter-dependent

Babuška inf-sup constant of the first-order optimality system, which is not only expensive in terms of computational cost but also involved in terms of implementation effort. We compare here the computational effort and performance, i.e., sharpness, of our proposed bounds with the bound from [29] when we discuss numerical results. We observe that our proposed bounds — in contrast to the bound from [29] — involve only constants (or their lower/upper bounds) that are straightforward and inexpensive to compute. Furthermore, numerical results show that the new bound derived from the error residual equations of the optimality system tends to be much sharper, especially in the case of optimal control problems involving small regularization parameters.

Although we consider a purely deterministic problem here, the input parameters could also be considered random inputs. We note that the approach presented here can be gainfully employed in such a stochastic setting, see for example [8] or [4]. For a more detailed comparison between the reduced basis method and stochastic collocation methods we refer to [5].

This paper is organized as follows. In Section 2 we introduce the finite element (truth) optimal control problem and state the first-order optimality conditions. The reduced basis approximation of the optimal control problem is illustrated in Section 3, where we also explain the associated offline-online computational procedure and briefly summarize the greedy procedure to generate the reduced basis spaces. In Section 4, we discuss the *a posteriori* error estimation procedures. We propose two new *a posteriori* error bounds for the optimal control and the associated cost functional before briefly reviewing the bound from [29]. Finally, we present numerical results for a Graetz flow problem and a heat transfer problem in Section 5 and offer concluding remarks in Section 6.

2 General problem statement and truth discretization

In this section we introduce the parametrized linear-quadratic optimal control problem with elliptic PDE constraint and distributed control. We introduce a finite element truth discretization for the exact, i.e., continuous problem and recall the first-order necessary (and in our case sufficient) optimality conditions.

2.1 Preliminaries

Let Y_e with $H_0^1(\Omega) \subset Y_e \subset H^1(\Omega)$ be a Hilbert space over the bounded Lipschitz domain $\Omega \subset \mathbb{R}^d$, $d = 1, 2, 3$, with boundary Γ .¹ The inner product and induced norm associated with Y_e are given by $(\cdot, \cdot)_Y$ and $\|\cdot\|_Y = \sqrt{(\cdot, \cdot)_Y}$, respectively. We assume that the norm $\|\cdot\|_Y$ is equivalent to the $H^1(\Omega)$ -norm and denote the dual space of Y_e by Y_e' . We also introduce the control Hilbert space U_e , together with its reference inner product $(\cdot, \cdot)_U$, induced reference norm $\|\cdot\|_U = \sqrt{(\cdot, \cdot)_U}$, and associated dual space U_e' .² Furthermore, let $\mathcal{D} \subset \mathbb{R}^P$ be a prescribed compact parameter set in which our parameter $\mu = (\mu_1, \dots, \mu_P)$ resides.

We directly consider a finite element approximation for the infinite-dimensional optimal control problem. To this end we define two conforming finite element spaces $Y \subset Y_e$ and $U \subset U_e$. We denote their typically large dimensions by $\mathcal{N}_Y = \dim(Y)$ and $\mathcal{N}_U = \dim(U)$. We shall assume that the truth spaces Y and U are sufficiently rich such that the finite element

¹ The subscripts “e” denote “exact”.

² Our framework covers spatially distributed controls $U_e = L^2(\Omega_U)$, $\Omega_U \subset \Omega$, and Neumann boundary controls $U_e = L^2(\Gamma_U)$, $\Gamma_U \subset \Gamma$. It also applies to finite-dimensional control spaces $U_e = \mathbb{R}^m$.

solutions guarantee a desired accuracy over the whole parameter domain \mathcal{D} . We further recall that the reduced basis approximation shall be built upon – and the reduced basis error thus evaluated with respect to – the truth solution $y(\mu) \in Y$ and $u(\mu) \in U$.

We next introduce the parameter-dependent bilinear form $a(\cdot, \cdot; \mu) : Y \times Y \rightarrow \mathbb{R}$, and shall assume that $a(\cdot, \cdot; \mu)$ is continuous,

$$0 < \gamma_a(\mu) = \sup_{w \in Y \setminus \{0\}} \sup_{v \in Y \setminus \{0\}} \frac{a(w, v; \mu)}{\|w\|_Y \|v\|_Y} \leq \gamma_0^a < \infty \quad \forall \mu \in \mathcal{D}, \quad (1)$$

and coercive,

$$\alpha_a(\mu) = \inf_{v \in Y \setminus \{0\}} \frac{a(v, v; \mu)}{\|v\|_Y^2} \geq \alpha_0^a > 0 \quad \forall \mu \in \mathcal{D}. \quad (2)$$

Furthermore we introduce the parameter-dependent continuous linear functional $f(\cdot; \mu) : Y \rightarrow \mathbb{R}$ and the parameter-dependent bilinear form $d(\cdot, \cdot; \mu) : Y \times Y \rightarrow \mathbb{R}$, where $d(\cdot, \cdot; \mu)$ is continuous, symmetric, and positive semi-definite and hence induces an associated semi-norm $|\cdot|_{D(\mu)} = \sqrt{d(\cdot, \cdot; \mu)}$. Furthermore $c(\cdot, \cdot; \mu) : U \times U \rightarrow \mathbb{R}$ is a parameter-dependent energy inner product on U . The associated induced energy norm is denoted by $\|\cdot\|_{U(\mu)} = \sqrt{c(\cdot, \cdot; \mu)}$ and we assume that it is equivalent to the reference norm $\|\cdot\|_U$ on U . In the following we will use the notation $(\cdot, \cdot)_{U(\mu)} := c(\cdot, \cdot; \mu)$ and $(\cdot, \cdot)_{D(\mu)} := d(\cdot, \cdot; \mu)$. We also introduce the parameter-dependent bilinear form $b(\cdot, \cdot; \mu) : U \times Y \rightarrow \mathbb{R}$ and assume that $b(\cdot, \cdot; \mu)$ is continuous,

$$0 < \gamma_b(\mu) = \sup_{w \in U \setminus \{0\}} \sup_{v \in Y \setminus \{0\}} \frac{b(w, v; \mu)}{\|w\|_{U(\mu)} \|v\|_Y} \leq \gamma_0^b < \infty \quad \forall \mu \in \mathcal{D}. \quad (3)$$

Finally, in anticipation of the optimal control problem defined in Section 2.2, we introduce the parametrized desired state $y_d(\mu) \in Y$.

The involved bilinear and linear forms as well as the desired state are assumed to depend affinely on the parameter, i.e., for all $w, v \in Y$, $u, z \in U$ and all parameters $\mu \in \mathcal{D}$,

$$\begin{aligned} a(w, v; \mu) &= \sum_{q=1}^{Q_a} \Theta_a^q(\mu) a^q(w, v), & b(u, v; \mu) &= \sum_{q=1}^{Q_b} \Theta_b^q(\mu) b^q(u, v), \\ d(w, v; \mu) &= \sum_{q=1}^{Q_d} \Theta_d^q(\mu) d^q(w, v), & c(u, z; \mu) &= \sum_{q=1}^{Q_c} \Theta_c^q(\mu) c^q(u, z), \\ f(v; \mu) &= \sum_{q=1}^{Q_f} \Theta_f^q(\mu) f^q(v), & y_d(x; \mu) &= \sum_{q=1}^{Q_{y_d}} \Theta_{y_d}^q(\mu) y_d^q(x), \end{aligned} \quad (4)$$

for some (preferably) small integers Q_a , Q_b , Q_c , Q_d , Q_f , and Q_{y_d} . Here, the coefficient functions $\Theta^q(\cdot) : \mathcal{D} \rightarrow \mathbb{R}$, are continuous and depend on μ , but the continuous bilinear forms $a^q(\cdot, \cdot) : Y \times Y \rightarrow \mathbb{R}$, $b^q(\cdot, \cdot) : U \times Y \rightarrow \mathbb{R}$, $d^q(\cdot, \cdot) : Y \times Y \rightarrow \mathbb{R}$, $c^q(\cdot, \cdot) : U \times U \rightarrow \mathbb{R}$, as well as the continuous linear forms $f^q : Y \rightarrow \mathbb{R}$ and $y_d^q \in Y$ do *not* depend on μ .

2.2 General problem statement

We consider the parametrized optimal control problem³

$$\begin{aligned} \min_{y \in Y, u \in U} J(y, u; \mu) &= \frac{1}{2} |y - y_d(\mu)|_{D(\mu)}^2 + \frac{\lambda}{2} \|u - u_d\|_{U(\mu)}^2 \\ \text{s.t. } (y, u) \in Y \times U &\text{ solves } a(y, v; \mu) = b(u, v; \mu) + f(v; \mu) \quad \forall v \in Y. \end{aligned} \quad (\text{P})$$

Here, $y_d(\mu) \in Y$, $\mu \in \mathcal{D}$ is the desired state and $u_d \in U$ is the desired control. The regularization parameter $\lambda > 0$ governs the trade-off between the cost associated with the deviation from the desired state and the desired control, respectively. For simplicity, we assume that the desired control u_d is parameter-independent; however, (affine) parameter dependence is readily admitted.

It follows from our assumptions that there exists a unique optimal solution (y^*, u^*) to (P); see e.g. [25]. By employing a Lagrangian approach, we obtain the first-order optimality system consisting of the state equation, the adjoint equation, and the optimality equation: Given $\mu \in \mathcal{D}$, the optimal solution $(y^*, p^*, u^*) \in Y \times Y \times U$ satisfies⁴

$$a(y^*, \phi; \mu) = b(u^*, \phi; \mu) + f(\phi; \mu) \quad \forall \phi \in Y, \quad (5a)$$

$$a(\varphi, p^*; \mu) = (y_d(\mu) - y^*, \varphi)_{D(\mu)} \quad \forall \varphi \in Y, \quad (5b)$$

$$\lambda (u^* - u_d, \psi)_{U(\mu)} - b(\psi, p^*; \mu) = 0 \quad \forall \psi \in U. \quad (5c)$$

Here, p is the adjoint variable and the superscript $*$ denotes optimality. We note that for the linear-quadratic optimal control problem (P) the first-order conditions (5) are necessary and sufficient for the optimality of (y^*, u^*) [25]. We also note that the trial and test spaces are identical for the state and adjoint equations. The “first-discretize-then-optimize” and “first-optimize-then-discretize” approaches commute in this setting and hence lead to the same discrete the optimality system (5), see for example [13].

The optimality system (5) constitutes a coupled set of equations of dimension $2\mathcal{N}_Y + \mathcal{N}_U$ and is thus expensive to solve, especially if one is interested in various values of $\mu \in \mathcal{D}$. Our goal is therefore to significantly speed up the solution of (5) by employing the reduced basis approximation as a surrogate model for the PDE constraint in (P).

Remark 1 In practice, the regularization parameter often serves as a design parameter which is tuned to achieve a desired performance of the optimal controller. From a reduced basis point of view, however, the regularization parameter may simply be considered an input parameter of the parametrized optimal control problem. This allows us to vary λ online and thus to efficiently design the optimal controller as discussed in the context of parabolic optimal control problems in [20].

Remark 2 In the sequel we derive the reduced basis approximation and associated *a posteriori* error bounds for the linear-quadratic setting (P). We note that the method can be easily extended to account for a general linear observation operator in the cost functional. However, the extension to control or state constrained problems is neither obvious nor straightforward, since determining the active and inactive sets requires an operation on the truth finite element grid. Furthermore, the extension to problems involving nonlinear PDE constraints poses several challenges, such as the development of certified reduced order approximation of the PDE itself; also see e.g. [17].

³ Here and in the following we often omit the dependence on μ to simplify notation.

⁴ We again note that we omit the dependence on μ to simplify notation, i.e., we write $y = y(\mu)$, $p = p(\mu)$, and $u = u(\mu)$.

3 Reduced basis approximation

We will now employ the reduced basis method for the efficient solution of the truth optimal control problem (P). We first assume that we are given the sample sets $\mathcal{D}_N = \{\mu^1, \dots, \mu^N\}$, $1 \leq N \leq N_{\max}$, and associated *integrated* reduced basis spaces

$$Y_N = \text{span}\{\zeta_n^y, 1 \leq n \leq 2N\} = \text{span}\{y^*(\mu^n), p^*(\mu^n), 1 \leq n \leq N\}, \quad 1 \leq N \leq N_{\max}, \quad (6)$$

where $y^*(\mu^n)$ and $p^*(\mu^n)$ are the solutions of (5) and ζ_n^y are mutually $(\cdot, \cdot)_Y$ -orthogonal basis functions derived by a Gram-Schmidt orthogonalization procedure. Note that we integrate both state and adjoint snapshots in Y_N ; thus the term “integrated.” We refer to [21, 20, 29] for further details and discussion on the use of integrated spaces for the state and adjoint equations. Furthermore we assume that the reduced basis control spaces are given by

$$U_N = \text{span}\{\zeta_n^u, 1 \leq n \leq N\} = \text{span}\{u^*(\mu^n), 1 \leq n \leq N\}, \quad 1 \leq N \leq N_{\max}. \quad (7)$$

Here, the ζ_n^u , $1 \leq n \leq N$, are mutually $(\cdot, \cdot)_U$ -orthogonal basis functions. We comment on the greedy sampling procedure to construct the spaces Y_N and U_N in Section 3.2. Although the snapshots generated by the greedy procedure can be linearly dependent, we will assume in the following $\dim(Y_N) = 2N$ and $\dim(U_N) = N$ to simplify the presentation.

We next replace the truth approximation of the PDE constraint in (P) by its reduced basis approximation. The reduced basis optimal control problem is thus given by

$$\begin{aligned} & \min_{y_N \in Y_N, u_N \in U_N} J(y_N, u_N; \mu) & (P_N) \\ \text{s.t. } & (y_N, u_N) \in Y_N \times U_N \quad \text{solves} \quad a(y_N, v; \mu) = b(u_N, v; \mu) + f(v; \mu) \quad \forall v \in Y_N. \end{aligned}$$

We can also directly state the associated first-order optimality system: Given $\mu \in \mathcal{D}$, find $(y_N^*, p_N^*, u_N^*) \in Y_N \times Y_N \times U_N$ such that

$$a(y_N^*, \phi; \mu) = b(u_N^*, \phi; \mu) + f(\phi; \mu) \quad \forall \phi \in Y_N, \quad (8a)$$

$$a(\varphi, p_N^*; \mu) = (y_d(\mu) - y_N^*, \varphi)_{D(\mu)} \quad \forall \varphi \in Y_N, \quad (8b)$$

$$\lambda (u_N^* - u_d, \psi)_{U(\mu)} - b(\psi, p_N^*; \mu) = 0 \quad \forall \psi \in U_N. \quad (8c)$$

The reduced basis optimality system is only of dimension $5N$ and can be evaluated efficiently using an offline-online computational decomposition. The details are presented in the following subsection.

We also note that we use a single reduced basis trial and test space for the state and adjoint equations. The reason is twofold: First, in this case the “first-reduce-then-optimize” and “first-optimize-then-reduce” approaches are equivalent. Second, using different spaces may result in an unstable system (8). This issue is closely related to the stability of reduced basis formulations for saddle point problems, see [10] for details. If we use the same space Y_N for the state *and* the adjoint equation, on the other hand, the system (8) is provably stable [27, 29]. Finally, since the state and adjoint solutions need to be well-approximated by the single space Y_N , we choose integrated spaces; see (6).

3.1 Computational procedure

We now turn to the computational details of the reduced basis approximation of the optimality system. To this end, we express the reduced basis state, adjoint and control solutions as $y_N(\mu) = \sum_{i=1}^{2N} y_{Ni}(\mu) \zeta_i^y$, $p_N(\mu) = \sum_{i=1}^{2N} p_{Ni}(\mu) \zeta_i^y$, and $u_N(\mu) = \sum_{i=1}^N u_{Ni}(\mu) \zeta_i^u$, and denote the coefficient vectors by $\underline{y}_N(\mu) = [y_{N1}(\mu), \dots, y_{N2N}(\mu)]^T \in \mathbb{R}^{2N}$, $\underline{p}_N(\mu) = [p_{N1}(\mu), \dots, p_{N2N}(\mu)]^T \in \mathbb{R}^{2N}$ and $\underline{u}_N(\mu) = [u_{N1}(\mu), \dots, u_{NN}(\mu)]^T \in \mathbb{R}^N$, respectively. If we choose as test functions $\phi = \zeta_i^y$, $1 \leq i \leq 2N$, $\varphi = \zeta_i^u$, $1 \leq i \leq N$, and $\psi = \zeta_i^u$, $1 \leq i \leq N$, the reduced basis optimality system (8) can be expressed in terms of the $5N \times 5N$ linear system

$$\begin{bmatrix} D_N(\mu) & 0 & A_N^T(\mu) \\ 0 & \lambda C_N(\mu) & -B_N^T(\mu) \\ A_N(\mu) & -B_N(\mu) & 0 \end{bmatrix} \begin{bmatrix} \underline{y}_N \\ \underline{p}_N \\ \underline{u}_N \end{bmatrix} = \begin{bmatrix} Y_{d,N}(\mu) \\ \lambda U_{d,N}(\mu) \\ F_N(\mu) \end{bmatrix}. \quad (9)$$

Here, we have reordered the variables and equations to exhibit the saddle point structure of the system. The matrices $A_N(\mu) \in \mathbb{R}^{2N \times 2N}$, $B_N(\mu) \in \mathbb{R}^{2N \times N}$, $D_N(\mu) \in \mathbb{R}^{2N \times 2N}$, and $C_N(\mu) \in \mathbb{R}^{N \times N}$ are defined by the entries $(A_N(\mu))_{ij} = a(\zeta_j^y, \zeta_i^y; \mu)$, $(B_N(\mu))_{ij} = b(\zeta_j^u, \zeta_i^y; \mu)$, $(D_N(\mu))_{ij} = d(\zeta_j^y, \zeta_i^y; \mu)$, and $(C_N(\mu))_{ij} = c(\zeta_j^u, \zeta_i^u; \mu)$, respectively. The vectors $F_N(\mu) \in \mathbb{R}^{2N}$, $Y_{d,N}(\mu) \in \mathbb{R}^{2N}$, and $U_{d,N}(\mu) \in \mathbb{R}^N$ are given by $(F_N(\mu))_i = f(\zeta_i^y; \mu)$, $(Y_{d,N}(\mu))_i = d(y_d(\mu), \zeta_i^y; \mu)$, and $(U_{d,N}(\mu))_i = c(u_d, \zeta_i^u; \mu)$, respectively.

The affine parameter dependence (4) yields the expansion $A_N(\mu) = \sum_{q=1}^{Q_a} \Theta_a^q(\mu) A_N^q$, where the parameter-independent matrices $A_N^q \in \mathbb{R}^{2N \times 2N}$ are given by $(A_N^q)_{ij} = a^q(\zeta_j^y, \zeta_i^y)$. The matrices $B_N(\mu)$, $D_N(\mu)$, $C_N(\mu)$ and vectors $F_N(\mu)$, $Y_{d,N}(\mu)$, and $U_{d,N}(\mu)$ yield a similar expansion. Finally, to allow an efficient evaluation of the cost functional in the online stage, we also save the three-dimensional tensor $Y_{d,d}$ given by $(Y_{d,d})_{q,p,r} = d^q(y_d^p, y_d^r)$, $1 \leq q \leq Q_d$, $1 \leq p \leq Q_{yd}$, $1 \leq r \leq Q_{yd}$, as well as the vector $(U_{d,d})_q = c^q(u_d, u_d)$, $1 \leq q \leq Q_c$.

The offline-online decomposition works as follows. In the offline stage — performed only *once* — we first construct the reduced basis spaces Y_N and U_N . We then assemble the parameter-independent quantities A_N^q ($1 \leq q \leq Q_a$), B_N^q ($1 \leq q \leq Q_b$), D_N^q ($1 \leq q \leq Q_d$), C_N^q ($1 \leq q \leq Q_c$), F_N^q ($1 \leq q \leq Q_f$), $Y_{d,N}^q$ ($1 \leq q \leq Q_d Q_{yd}$), $U_{d,N}^q$ ($1 \leq q \leq Q_c$), $Y_{d,d}$ and $U_{d,d}$. The computational cost clearly depends on the truth finite element dimensions \mathcal{N}_Y and \mathcal{N}_U . In the online stage — for each new parameter value μ — we first assemble all parameter-dependent quantities in (to leading order) $(Q_a + Q_b + Q_c + Q_d)N^2 + (Q_f + Q_d Q_{yd})N + Q_d Q_{yd}^2$ operations. We then solve the reduced basis optimality system (9) at cost $\mathcal{O}((5N)^3)$. Given the reduced basis optimal solution, the cost functional can then be evaluated efficiently from

$$\begin{aligned} J(y_N, u_N; \mu) &= \frac{1}{2} \left(\underline{y}_N^T D_N(\mu) \underline{y}_N - 2 \underline{y}_N^T Y_{d,N}(\mu) \underline{u}_N + Y_{d,d}(\mu) \right) \\ &\quad + \frac{\lambda}{2} \left(\underline{u}_N^T C_N(\mu) \underline{u}_N - 2 \underline{u}_N^T U_{d,N}(\mu) \underline{u}_N + U_{d,d}(\mu) \right), \end{aligned} \quad (10)$$

where we assemble $Y_{d,d}(\mu) = \sum_{q=1}^{Q_d} \sum_{p=1}^{Q_{yd}} \sum_{r=1}^{Q_{yd}} \Theta_d^q(\mu) \Theta_{yd}^p(\mu) \Theta_{yd}^r(\mu) (Y_{d,d})_{q,p,r}$ and $U_{d,d}(\mu) = \sum_{q=1}^{Q_c} \Theta_c^q(\mu) (U_{d,d})_q$. The computational cost for the cost functional evaluation is $\mathcal{O}(Q_d N^2 + Q_d Q_{yd} N + Q_d Q_{yd}^2)$ for the state misfit term plus $\mathcal{O}(Q_c N^2)$ for the control misfit term. Hence, the overall computational cost for the online stage is independent of \mathcal{N}_Y and \mathcal{N}_U , the dimensions of the underlying truth finite element approximation spaces. Since $N \ll \mathcal{N}_Y$ and $N \ll \mathcal{N}_U$, we expect a significant computational speed-up in the online stage relative to the solution of (5). However, we need to rigorously and efficiently assess the error introduced.

3.2 Greedy algorithm

We generate the reduced basis space using the greedy sampling procedure [36] summarized in Algorithm 1. To this end, we presume the existence of an *a posteriori* error bound $\Delta_N(\mu)$ — to be introduced in the next section — for the optimal control or the associated cost functional. Furthermore, $\Xi_{\text{train}} \subset \mathcal{D}$ is a finite but suitably large parameter train sample; $\mu^1 \in \Xi_{\text{train}}$ is the initial parameter value; and $\varepsilon_{\text{tol},\min} > 0$ is a prescribed error tolerance. Since we can only guarantee the desired error tolerance for all $\mu \in \Xi_{\text{train}}$, we note that we have to choose the train sample sufficiently fine. The reduced basis space Y_N is expanded in step 6 with a snapshot of the corresponding truth state and adjoint equation, i.e., we use “integrated” spaces as discussed previously. Simultaneously we reduce the control space, i.e., U_N is spanned by snapshots of the truth optimal control at the selected parameter values. Note that in step 6 and 7 we need to check if the new snapshots are already contained in the reduced basis spaces and consequently discard linear dependent snapshots. Although the reduced basis spaces could be of smaller dimension, we will assume $\dim(Y_N) = 2N$ and $\dim(U_N) = N$ to simplify the presentation. This is true for all numerical examples presented in Section 5.

Algorithm 1 Greedy Sampling Procedure

- 1: Choose $\Xi_{\text{train}} \subset \mathcal{D}$, $\mu^1 \in \Xi_{\text{train}}$, and $\varepsilon_{\text{tol},\min} > 0$
 - 2: Set $N \leftarrow 0$, $Y_N \leftarrow \{\}$, $U_N \leftarrow \{\}$
 - 3: Set $\mu^* \leftarrow \mu^1$ and $\Delta_N(\mu^*) \leftarrow \infty$
 - 4: **while** $\Delta_N(\mu^*) > \varepsilon_{\text{tol},\min}$ **do**
 - 5: $N \leftarrow N + 1$
 - 6: $Y_N \leftarrow Y_{N-1} \cup \text{span}\{y(\mu^*), p(\mu^*)\}$
 - 7: $U_N \leftarrow U_{N-1} \cup \text{span}\{u(\mu^*)\}$
 - 8: $\mu^* \leftarrow \arg \max_{\mu \in \Xi_{\text{train}}} \Delta_N(\mu)$
 - 9: **end while**
 - 10: $N_{\text{max}} \leftarrow N$
-

4 A posteriori error estimation

We next turn to the *a posteriori* error estimation procedure. We consider three different error bounds for the optimal control in Section 4.2 and subsequently derive associated cost functional error bounds in Section 4.3. The error bounds introduced are rigorous upper bounds for the errors and are online-efficient to compute; we summarize the computational procedure in Section 4.4.

4.1 Preliminaries

To begin, we assume that we are given a positive lower bound $\alpha_a^{\text{LB}}(\mu) : \mathcal{D} \rightarrow \mathbb{R}_+$ for the coercivity constant $\alpha_a(\mu)$ defined in (2) such that

$$0 < \alpha_0^a \leq \alpha_a^{\text{LB}}(\mu) \leq \alpha_a(\mu) \quad \forall \mu \in \mathcal{D}. \quad (11)$$

Furthermore, we assume that we have upper bounds available for the constant

$$C_D^{\text{UB}}(\mu) \geq C_D(\mu) := \sup_{v \in Y \setminus \{0\}} \frac{|v|_{D(\mu)}}{\|v\|_Y} \geq 0 \quad \forall \mu \in \mathcal{D}, \quad (12)$$

and the continuity constant of the bilinear form $b(\cdot, \cdot; \mu)$

$$\gamma_b^{\text{UB}}(\mu) \geq \gamma_b(\mu) \quad \forall \mu \in \mathcal{D}. \quad (13)$$

It is possible to compute these constants (or their bounds) efficiently in terms of an offline-online procedure; see Section 4.4 for details. We also require the following definition.

Definition 1 The residuals of the state equation, the adjoint equation, and the optimality equation are defined by

$$r_y(\phi; \mu) = f(\phi; \mu) + b(u_N^*, \phi; \mu) - a(y_N^*, \phi; \mu) \quad \forall \phi \in Y, \quad \forall \mu \in \mathcal{D}, \quad (14)$$

$$r_p(\varphi; \mu) = (y_d(\mu) - y_N^*, \varphi)_{D(\mu)} - a(\varphi, p_N^*; \mu) \quad \forall \varphi \in Y, \quad \forall \mu \in \mathcal{D}, \quad (15)$$

$$r_u(\psi; \mu) = b(\psi, p_N^*; \mu) - \lambda (u_N^* - u_d, \psi)_{U(\mu)} \quad \forall \psi \in U, \quad \forall \mu \in \mathcal{D}. \quad (16)$$

4.2 Control error bounds

We now introduce two new *a posteriori* error bounds for the optimal control: the first is based on a perturbation approach proposed in [35] and the second is directly derived from the error residual equations of the optimality system. At the end of this section, we briefly recall a previously proposed bound based on the Banach-Nečas-Babuška (BNB) theory [9].

4.2.1 Perturbation approach (PER)

The perturbation approach was originally proposed in [35] for POD approximations to optimal control problems. As pointed out previously, evaluation of the error bound introduced in [35] requires a “forward-backward” truth solution and is thus computationally expensive. Based on this work, we developed rigorous *and* efficient reduced basis control error bounds in different contexts, i.e., for elliptic problems with scalar controls in [11, 21] and for parabolic problems in [20]. Here, we extend this work to problems involving distributed controls, also see [18]. The derivation is based on the following result from [35] (see Theorem 3.1 therein for the proof).

Theorem 1 Let u^* and u_N^* be the optimal solutions to the truth and reduced basis optimal control problems (P) and (P_N), respectively. The error in the optimal control then satisfies

$$\|u^* - u_N^*\|_{U(\mu)} \leq \Delta_N^{u, \text{TV}}(\mu) := \frac{1}{\lambda} \|\lambda(u_N^* - u_d) - \mathcal{B}^* p(y(u_N^*))\|_{U(\mu)} \quad \forall \mu \in \mathcal{D}, \quad (17)$$

where $\mathcal{B}^* : Y \rightarrow U$ is the adjoint operator⁵ defined by

$$b(\psi, \phi; \mu) = (\psi, \mathcal{B}^* \phi)_{U(\mu)} \quad \forall \psi \in U, \phi \in Y, \quad \forall \mu \in \mathcal{D}. \quad (18)$$

Note that the error bound measures the error in the energy control norm $\|\cdot\|_{U(\mu)}$, which is the more relevant norm for parametrized geometries. In such a case we perform an affine mapping from the parameter-dependent geometry to a parameter-independent reference geometry. This results in a parameter-dependent inner product and induced norm on the control space U [32]. Furthermore, we assume that the adjoint operator \mathcal{B}^* itself is parameter-independent, i.e., the parameter-dependence of $b(\cdot, \cdot; \mu)$ is caused only by the presence of the parameter-dependent inner product $(\cdot, \cdot)_{U(\mu)}$ in (18). This assumption is satisfied by all numerical examples in this paper. Nevertheless, an extension to parameter-dependent \mathcal{B}^* is possible in many cases (see [19] for more details). In order to derive the error bound in the following, we must compute the parameter-dependent constant (or an upper bound)

$$\|\mathcal{B}^*\|_{Y \rightarrow U(\mu)} := \sup_{\phi \in Y \setminus \{0\}} \frac{\|\mathcal{B}^* \phi\|_{U(\mu)}}{\|\phi\|_Y}, \quad (19)$$

such that $\|\mathcal{B}^* \phi\|_{U(\mu)} \leq \|\mathcal{B}^*\|_{Y \rightarrow U(\mu)} \|\phi\|_Y$ holds for all $\phi \in Y$. From the definition of the adjoint operator in (18) and the Cauchy-Schwarz inequality it follows that

$$\|\mathcal{B}^* \phi\|_{U(\mu)} = \sup_{\psi \in U \setminus \{0\}} \frac{(\mathcal{B}^* \phi, \psi)_{U(\mu)}}{\|\psi\|_{U(\mu)}} = \sup_{\psi \in U \setminus \{0\}} \frac{b(\psi, \phi; \mu)}{\|\psi\|_{U(\mu)}}. \quad (20)$$

Hence by the definition of $\gamma_b(\mu)$ in (3) we obtain that $\|\mathcal{B}^*\|_{Y \rightarrow U(\mu)} = \gamma_b(\mu)$.

We further note that $y(u_N^*)$ is the solution of the (truth) state equation (5a) with control u_N^* instead of u^* , and $p(y(u_N^*))$ is the solution of the (truth) adjoint equation (5b) with $y(u_N^*)$ instead of $y^*(u^*)$ on the right-hand side. Evaluation of the bound (17) thus requires a consecutive solution of both the state and adjoint truth approximations and is computationally expensive. In contrast, the bound developed in the following is online-efficient, i.e., its evaluation is independent of \mathcal{N}_Y and \mathcal{N}_U . The underlying idea is to replace the truth approximation $p(y(u_N^*))$ in (17) with the reduced basis approximation $p_N^*(y_N^*(u_N^*))$ and to bound the error term $p(y(u_N^*)) - p_N^*(y_N^*(u_N^*))$.

Before we continue, let us make some notational remarks. Following the notation and terminology in [7], we refer to $\tilde{e}^y = y(u_N^*) - y_N^*(u_N^*)$ as the state predictability error and to $\tilde{e}^p = p(y(u_N^*)) - p_N^*(y_N^*(u_N^*))$ as the adjoint predictability error. They reflect the ability of the corresponding reduced basis solutions to approximate the truth state and adjoint solutions for a prescribed control. We further define the state, adjoint, and control optimality errors as $e^{y,*} = y^*(u^*) - y_N^*(u_N^*)$, $e^{p,*} = p^*(y^*(u^*)) - p_N^*(y_N^*(u_N^*))$, and $e^{u,*} = u^* - u_N^*$, respectively. Before turning to the bound for the optimal control we require two intermediate results for the state and adjoint predictability errors.

Lemma 1 *The state predictability error, $\tilde{e}^y = y(u_N^*) - y_N^*(u_N^*)$, is bounded by*

$$\|\tilde{e}^y\|_Y \leq \tilde{\Delta}_N^y(\mu) := \frac{\|r_y(\cdot; \mu)\|_{Y'}}{\alpha_a^{\text{LB}}(\mu)} \quad \forall \mu \in \mathcal{D}, \quad (21)$$

where $y_N^*(u_N^*)$ is the solution of (8a) and $y(u_N^*)$ is the solution of the truth state equation (5a) with control u_N^* .

⁵ The bilinear form $b(\cdot, \cdot; \mu) : U \times Y \rightarrow \mathbb{R}$ defines an associated mapping $\mathcal{B}(\mu) : U \rightarrow Y'$ given by $\langle \mathcal{B}(\mu)\psi, \phi \rangle_{Y', Y} = b(\psi, \phi; \mu)$ for all $\psi \in U, \phi \in Y, \mu \in \mathcal{D}$.

This is the standard *a posteriori* error bound for coercive elliptic PDEs [30].

Lemma 2 *The adjoint predictability error, $\tilde{e}^p = p(y(u_N^*)) - p_N^*(y_N^*(u_N^*))$, is bounded by*

$$\|\tilde{e}^p\|_Y \leq \tilde{\Delta}_N^p(\mu) := \frac{1}{\alpha_a^{\text{LB}}(\mu)} (\|r_p(\cdot; \mu)\|_{Y'} + C_D^{\text{UB}}(\mu)^2 \tilde{\Delta}_N^y(\mu)) \quad \forall \mu \in \mathcal{D}, \quad (22)$$

where $p_N^*(y_N^*(u_N^*))$ is the solution of (8b) and $p(y(u_N^*))$ is the solution of the truth adjoint equation (5b) with $y(u_N^*)$ on the right-hand side.

Proof We note from (15) and (5b) that the error, \tilde{e}^p , satisfies

$$a(\varphi, \tilde{e}^p; \mu) = r_p(\varphi; \mu) + (y_N^*(u_N^*) - y(u_N^*), \varphi)_{D(\mu)} \quad \forall \varphi \in Y. \quad (23)$$

We now choose $\varphi = \tilde{e}^p$ and invoke (2), (11), the definition of the dual norm of the residual, and the Cauchy-Schwarz inequality to obtain

$$\alpha_a^{\text{LB}}(\mu) \|\tilde{e}^p\|_Y^2 \leq \|r_p(\cdot; \mu)\|_{Y'} \|\tilde{e}^p\|_Y + |y(u_N^*) - y_N^*(u_N^*)|_{D(\mu)} |\tilde{e}^p|_{D(\mu)}. \quad (24)$$

The desired result directly follows from the definition of $C_D(\mu)$ and Lemma 1.

We note that this proof is in fact a simple extension of the proof of the standard error bound. The main difference is the additional error term due to the change in the right-hand sides of equations (5b) and (8b). We are now ready to state the optimal control error bound.

Proposition 1 *Let u^* and u_N^* be the optimal solutions of the truth and reduced basis optimal control problems, respectively. Given $\tilde{\Delta}_N^p(\mu)$ defined in (22), the error in the optimal control satisfies*

$$\begin{aligned} \|u^* - u_N^*\|_{U(\mu)} \leq \Delta_N^{u, \text{PER}}(\mu) &:= \frac{1}{\lambda} \|\lambda(u_N^* - u_d) - \mathcal{B}^* p_N^*\|_{U(\mu)} \\ &+ \frac{1}{\lambda} \gamma_b^{\text{UB}}(\mu) \tilde{\Delta}_N^p(\mu) \quad \forall \mu \in \mathcal{D}. \end{aligned} \quad (25)$$

Proof We append $\pm \mathcal{B}^* p_N^*(y_N^*(u_N^*))$ to the bound in (17) and invoke the triangle inequality to obtain for all $\mu \in \mathcal{D}$

$$\|u^* - u_N^*\|_{U(\mu)} \leq \frac{1}{\lambda} \|\lambda(u_N^* - u_d) - \mathcal{B}^* p_N^*\|_{U(\mu)} + \frac{1}{\lambda} \|\mathcal{B}^*(p_N^* - p(y(u_N^*)))\|_{U(\mu)}. \quad (26)$$

The desired result directly follows from the definition of the constant $\|\mathcal{B}^*\|_{Y \rightarrow U(\mu)} = \gamma_b(\mu)$ and Lemma 2.

4.2.2 Alternative approach (ALT)

Here, we present a second new approach for the construction of a control error bound, which is based on a direct manipulation of the error residual equations of the optimality system. We will denote this bound — for lack of a better name — by ALT, for “alternative”. As for the perturbation approach, the bound measures the error in the energy control norm $\|\cdot\|_{U(\mu)}$.

Proposition 2 Let u^* and u_N^* be the optimal solutions to the truth and reduced basis optimal control problems, respectively. For any given parameter $\mu \in \mathcal{D}$, the error in the optimal control satisfies

$$\|u^* - u_N^*\|_{U(\mu)} \leq \Delta_N^{u,\text{ALT}}(\mu), \quad (27)$$

where $\Delta_N^{u,\text{ALT}}(\mu) := c_1(\mu) + \sqrt{c_1(\mu)^2 + c_2(\mu)}$ with nonnegative coefficients

$$c_1(\mu) = \frac{1}{2\lambda} \left(\|r_u(\cdot; \mu)\|_{U(\mu)'} + \frac{\gamma_b^{\text{UB}}(\mu)}{\alpha_a^{\text{LB}}(\mu)} \|r_p(\cdot; \mu)\|_{Y'} \right), \quad (28)$$

$$c_2(\mu) = \frac{1}{\lambda} \left[\frac{2}{\alpha_a^{\text{LB}}(\mu)} \|r_y(\cdot; \mu)\|_{Y'} \|r_p(\cdot; \mu)\|_{Y'} + \frac{1}{4} \left(\frac{C_D^{\text{UB}}(\mu)}{\alpha_a^{\text{LB}}(\mu)} \|r_y(\cdot; \mu)\|_{Y'} \right)^2 \right]. \quad (29)$$

Although this error bound looks admittedly complicated, we note that it only contains the dual norms of the state, adjoint, and optimality equation residuals which also appear in the previous two bounds. Furthermore, it only depends on constants or rather on their lower/upper bounds, which are straightforward to compute. We also note that, overall, terms involving the dual norm of the state residual, $\|r_y(\cdot; \mu)\|_{Y'}$, scale with $1/\sqrt{\lambda}$, whereas all other terms scale with $1/\lambda$. This is in contrast to the perturbation approach of the last section. Usually, small values of λ allow for a better fit of the optimal state y^* to the desired state $y_d(\mu)$. Since the difference $(y_d(\mu) - y^*, \cdot)_{D(\mu)}$ acts as a source term for the adjoint equation, a small misfit will typically result in a p^* of small norm compared to y^* ; in this case $\|r_y(\cdot; \mu)\|_{Y'}$ will dominate $\|r_p(\cdot; \mu)\|_{Y'}$. As a result, we expect the bound (27) to perform better than (25) for small regularization parameters λ . We will confirm this observation in the numerical results in Section 5. We turn to the proof of Proposition 2.

Proof We start from the error residual equations

$$a(e^{y^*}, \phi; \mu) - b(e^{u^*}, \phi; \mu) = r_y(\phi; \mu) \quad \forall \phi \in Y, \quad (30)$$

$$a(\varphi, e^{p^*}; \mu) + (e^{y^*}, \varphi)_{D(\mu)} = r_p(\varphi; \mu) \quad \forall \varphi \in Y, \quad (31)$$

$$\lambda(e^{u^*}, \psi)_{U(\mu)} - b(\psi, e^{p^*}; \mu) = r_u(\psi; \mu) \quad \forall \psi \in U. \quad (32)$$

From (30) with $\phi = e^{y^*}$ we obtain

$$\alpha_a^{\text{LB}}(\mu) \|e^{y^*}\|_Y^2 \leq a(e^{y^*}, e^{y^*}; \mu) = r_y(e^{y^*}; \mu) + b(e^{u^*}, e^{y^*}; \mu), \quad (33)$$

and therefore (as in Lemma 3)

$$\|e^{y^*}\|_Y \leq \frac{1}{\alpha_a^{\text{LB}}(\mu)} (\|r_y(\cdot; \mu)\|_{Y'} + \gamma_b(\mu) \|e^{u^*}\|_{U(\mu)}). \quad (34)$$

Similarly, equation (31) with $\varphi = e^{p^*}$ yields

$$\alpha_a^{\text{LB}}(\mu) \|e^{p^*}\|_Y^2 \leq a(e^{p^*}, e^{p^*}; \mu) = r_p(e^{p^*}; \mu) - (e^{y^*}, e^{p^*})_{D(\mu)}, \quad (35)$$

and thus (similar to in Lemma 4)

$$\|e^{p^*}\|_Y \leq \frac{1}{\alpha_a^{\text{LB}}(\mu)} (\|r_p(\cdot; \mu)\|_{Y'} + C_D(\mu) |e^{y^*}|_{D(\mu)}). \quad (36)$$

Choosing the test functions $\phi = e^{P,*}$, $\varphi = e^{Y,*}$, and $\psi = e^{U,*}$ in equations (30) – (32), we obtain

$$a(e^{Y,*}, e^{P,*}; \mu) - b(e^{U,*}, e^{P,*}; \mu) = r_y(e^{P,*}; \mu), \quad (37)$$

$$a(e^{Y,*}, e^{P,*}; \mu) + (e^{Y,*}, e^{Y,*})_{D(\mu)} = r_p(e^{Y,*}; \mu), \quad (38)$$

$$\lambda(e^{U,*}, e^{U,*})_{U(\mu)} - b(e^{U,*}, e^{P,*}; \mu) = r_u(e^{U,*}; \mu). \quad (39)$$

Adding (38) and (39) and subtracting (37) yields

$$\lambda(e^{U,*}, e^{U,*})_{U(\mu)} + (e^{Y,*}, e^{Y,*})_{D(\mu)} = -r_y(e^{P,*}; \mu) + r_p(e^{Y,*}; \mu) + r_u(e^{U,*}; \mu) \quad (40)$$

and hence

$$\begin{aligned} \lambda \|e^{U,*}\|_{U(\mu)}^2 + |e^{Y,*}|_{D(\mu)}^2 &\leq \|r_y(\cdot; \mu)\|_{Y'} \|e^{P,*}\|_Y + \|r_p(\cdot; \mu)\|_{Y'} \|e^{Y,*}\|_Y \\ &\quad + \|r_u(\cdot; \mu)\|_{U(\mu)} \|e^{U,*}\|_{U(\mu)}. \end{aligned} \quad (41)$$

We now plug (34) and (36) in (41) to obtain

$$\begin{aligned} \lambda \|e^{U,*}\|_{U(\mu)}^2 + |e^{Y,*}|_{D(\mu)}^2 &\leq \|r_u(\cdot; \mu)\|_{U(\mu)} \|e^{U,*}\|_{U(\mu)} \\ &\quad + \frac{1}{\alpha_a^{\text{LB}}(\mu)} \|r_p(\cdot; \mu)\|_{Y'} (\|r_y(\cdot; \mu)\|_{Y'} + \gamma_b(\mu)) \|e^{U,*}\|_{U(\mu)} \\ &\quad + \frac{1}{\alpha_a^{\text{LB}}(\mu)} \|r_y(\cdot; \mu)\|_{Y'} (\|r_p(\cdot; \mu)\|_{Y'} + C_D(\mu)) |e^{Y,*}|_{D(\mu)}. \end{aligned} \quad (42)$$

Furthermore it follows from Young's inequality that

$$\frac{C_D(\mu)}{\alpha_a^{\text{LB}}(\mu)} \|r_y(\cdot; \mu)\|_{Y'} |e^{Y,*}|_{D(\mu)} \leq \frac{C_D(\mu)^2}{4\alpha_a^{\text{LB}}(\mu)^2} \|r_y(\cdot; \mu)\|_{Y'}^2 + |e^{Y,*}|_{D(\mu)}^2. \quad (43)$$

Combining the last two inequalities, rearranging terms and employing the upper bounds for the constants in (12) and (13) results in

$$\begin{aligned} \lambda \|e^{U,*}\|_{U(\mu)}^2 &\leq \|r_u(\cdot; \mu)\|_{U(\mu)} \|e^{U,*}\|_{U(\mu)} + \frac{2}{\alpha_a^{\text{LB}}(\mu)} \|r_y(\cdot; \mu)\|_{Y'} \|r_p(\cdot; \mu)\|_{Y'} \\ &\quad + \frac{\gamma_b^{\text{UB}}(\mu)}{\alpha_a^{\text{LB}}(\mu)} \|r_p(\cdot; \mu)\|_{Y'} \|e^{U,*}\|_{U(\mu)} + \frac{C_D^{\text{UB}}(\mu)^2}{4\alpha_a^{\text{LB}}(\mu)^2} \|r_y(\cdot; \mu)\|_{Y'}^2. \end{aligned} \quad (44)$$

Finally, we can formulate the last inequality as a quadratic inequality in $\|e^{U,*}\|_{U(\mu)}$,

$$\|e^{U,*}\|_{U(\mu)}^2 - 2c_1(\mu) \|e^{U,*}\|_{U(\mu)} - c_2(\mu) \leq 0, \quad (45)$$

and hence $\|e^{U,*}\|_{U(\mu)}$ is bounded by the larger root given by $\Delta_N^{u,\text{ALT}}(\mu)$.

4.2.3 Banach-Nečas-Babuška approach (BNB)

We now briefly recall a bound based on the Banach-Nečas-Babuška (BNB) theory [9], which was first used in [36] for reduced basis approximations to noncoercive problems, and in [29] in the context of optimal control problems. We summarize the main result from [29] here, because we compare the BNB-bound with our two new bounds in the next section.

For $x = (y, u, p) \in X = Y \times U \times Y$ and $\vartheta = (\varphi, \psi, \phi) \in X$, we introduce the bilinear form $K(\cdot, \cdot; \mu) : X \times X \rightarrow \mathbb{R}$ and the linear functional $F(\cdot; \mu) : X \rightarrow \mathbb{R}$ as

$$\begin{aligned} K(x, \vartheta; \mu) &= a(y, \phi; \mu) - b(u, \phi; \mu) + a(\varphi, p; \mu) + (y, \varphi)_{D(\mu)} + \lambda (u, \psi)_{U(\mu)} - b(\psi, p; \mu), \\ F(\vartheta; \mu) &= f(\phi; \mu) + (y_d(\mu), \varphi)_{D(\mu)} + \lambda (u_d, \psi)_{U(\mu)}. \end{aligned} \quad (46)$$

We can then express (5) compactly via: find $x^* \in X$ such that

$$K(x^*, \vartheta; \mu) = F(\vartheta; \mu) \quad \forall \vartheta \in X. \quad (47)$$

For the optimal reduced basis solution $x_N^* = (y_N^*, u_N^*, p_N^*)$ of (8), the corresponding residual is given by

$$r_x(\vartheta; \mu) = F(\vartheta; \mu) - K(x_N^*, \vartheta; \mu) = r_y(\phi; \mu) + r_p(\varphi; \mu) + r_u(\psi; \mu) \quad \forall \vartheta \in X. \quad (48)$$

We now have all necessary ingredients and can state the standard BNB-bound (see [36, 33] for a proof).

Proposition 3 *Let x^* and x_N^* be the optimal solutions to the truth and reduced basis optimal control problems, respectively. The error in the optimal triple satisfies*

$$\|x^* - x_N^*\|_X \leq \Delta_N^{x, \text{BNB}}(\mu) := \frac{\|r_x(\cdot; \mu)\|_{X'}}{\beta_{\text{Ba}}^{\text{LB}}(\mu)} \quad \forall \mu \in \mathcal{D}, \quad (49)$$

where $\beta_{\text{Ba}}^{\text{LB}}(\mu)$ is a lower bound of the inf-sup constant

$$\beta_{\text{Ba}}(\mu) = \inf_{\vartheta \in X \setminus \{0\}} \sup_{x \in X \setminus \{0\}} \frac{K(x; \vartheta; \mu)}{\|x\|_X \|\vartheta\|_X}, \quad (50)$$

and $\|\cdot\|_X$ is a given norm on X .

We make several remarks. First, we note that this is simply the standard result for reduced basis approximations of noncoercive problems [36], which was applied in [29] for reduced basis approximations of parametrized optimal control problems. Second, there is a certain freedom of choice on how to define the inner product and associated norm on X ; we specify and compare two options when discussing numerical results in Section 5. Third, since $\|u^* - u_N^*\|_U \leq C_{U, X} \|x^* - x_N^*\|_X$, the bound $\Delta_N^{x, \text{BNB}}(\mu)$ can also be used to bound the error in the optimal control. We thus define $\Delta_N^{u, \text{BNB}}(\mu) := C_{U, X} \Delta_N^{x, \text{BNB}}(\mu)$ for notational convenience. Finally, the computation of a lower bound of the inf-sup constant $\beta_{\text{Ba}}(\mu)$ requires large offline effort as noted in [29].

4.3 Cost functional error bounds

Given the error bounds for the optimal triple $x^* \in X$ and the optimal control $u^* \in U$, we may readily derive a bound for the error in the cost functional. After presenting the results for the PER- and ALT-approach, we review the BNB result.

4.3.1 Perturbation and alternative approach

For the PER- and ALT-approaches, we have derived only the a posteriori error bounds for the control so far. In order to formulate the error bound for the cost functional, we also require a posteriori error bounds associated with the optimal state and adjoint. These are stated in the following two preparatory lemmata. We note that the proofs of these lemmata are similar to the proof of Lemma 2, i.e., the error in the optimal control — or, more precisely, the error bound of the optimal control — propagates and appears as an additional term in the state and adjoint optimality error bounds.

Lemma 3 *The state optimality error, $e^{y,*} = y^*(u^*) - y_N^*(u_N^*)$, is bounded by*

$$\|e^{y,*}\|_Y \leq \Delta_N^{y,*}(\mu) := \frac{1}{\alpha_a^{\text{LB}}(\mu)} (\|r_y(\cdot; \mu)\|_{Y'} + \gamma_b^{\text{UB}}(\mu) \Delta_N^{u,*}(\mu)) \quad \forall \mu \in \mathcal{D}, \quad (51)$$

where $\bullet \in \{\text{PER}, \text{ALT}\}$.

Proof We note from (14) and (5a) that the error, $e^{y,*}$, satisfies

$$a(e^{y,*}, \phi; \mu) = r_y(\phi; \mu) + b(u^* - u_N^*, \phi; \mu) \quad \forall \phi \in Y. \quad (52)$$

We now choose $\phi = e^{y,*}$ and invoke (2), (11), and the definition of the dual norm of the residual to obtain

$$\alpha_a^{\text{LB}}(\mu) \|e^{y,*}\|_Y^2 \leq \|r_y(\cdot; \mu)\|_{Y'} \|e^{y,*}\|_Y + b(u^* - u_N^*, e^{y,*}; \mu). \quad (53)$$

From the definition of $\gamma_b(\mu)$ and by invoking respectively Proposition 1 and Proposition 2, we obtain the desired result.

Lemma 4 *The adjoint optimality error, $e^{p,*} = p^*(y^*(u^*)) - p_N^*(y_N^*(u_N^*))$, is bounded by*

$$\|e^{p,*}\|_Y \leq \Delta_N^{p,*}(\mu) := \frac{1}{\alpha_a^{\text{LB}}(\mu)} (\|r_p(\cdot; \mu)\|_{Y'} + C_D^{\text{UB}}(\mu)^2 \Delta_N^{y,*}(\mu)) \quad \forall \mu \in \mathcal{D}, \quad (54)$$

where $\bullet \in \{\text{PER}, \text{ALT}\}$.

The proof is analogous to the proof of Lemma 2 and therefore omitted. We can now state the cost functional error bound.

Proposition 4 *Let $J^* = J(y^*, u^*; \mu)$ and $J_N^* = J(y_N^*, u_N^*; \mu)$ be the optimal values of the cost functionals of the truth and reduced basis optimal control problems, respectively. The error then satisfies for all $\mu \in \mathcal{D}$*

$$|J^* - J_N^*| \leq \Delta_N^{J,*}(\mu) := \frac{1}{2} (\|r_y(\cdot; \mu)\|_{Y'} \Delta_N^{p,*}(\mu) + \|r_p(\cdot; \mu)\|_{Y'} \Delta_N^{y,*}(\mu) + \|r_u(\cdot; \mu)\|_{U(\mu')} \Delta_N^{u,*}(\mu)), \quad (55)$$

where $\bullet \in \{\text{PER}, \text{ALT}\}$.

Proof We use the standard result from [3] to bound the cost functional error by

$$\begin{aligned} |J^* - J_N^*| &= \frac{1}{2} r_x(e^{x,*}; \mu) = \frac{1}{2} (r_y(e^{p,*}; \mu) + r_p(e^{y,*}; \mu) + r_u(e^{u,*}; \mu)) \\ &\leq \frac{1}{2} (\|r_y(\cdot; \mu)\|_{Y'} \|e^{p,*}\|_Y + \|r_p(\cdot; \mu)\|_{Y'} \|e^{y,*}\|_Y + \|r_u(\cdot; \mu)\|_{U(\mu')} \|e^{u,*}\|_{U(\mu)}) \end{aligned} \quad (56)$$

for all $\mu \in \mathcal{D}$. The result follows from Lemma 3 and 4 and Proposition 1 respectively 2.

4.3.2 Banach-Nečas-Babuška approach

The cost functional error bound is defined in the next proposition.

Proposition 5 *Let $J^* = J(y^*, u^*; \mu)$ and $J_N^* = J(y_N^*, u_N^*; \mu)$ be the optimal values of the cost functionals of the truth and reduced basis optimal control problems, respectively. The error then satisfies*

$$|J^* - J_N^*| \leq \Delta_N^{J,\text{BNB}}(\mu) := \frac{1}{2} \frac{\|r_x(\cdot; \mu)\|_{X'}^2}{\beta_{\text{Ba}}^{\text{LB}}(\mu)} \quad \forall \mu \in \mathcal{D}. \quad (57)$$

Proof We use the standard result from [3] to estimate the error in the cost functional by

$$|J^* - J_N^*| = \frac{1}{2} r_x(e^{x^*}; \mu) \leq \frac{1}{2} \|r_x(\cdot; \mu)\|_{X'} \|e^{x^*}\|_X \quad \forall \mu \in \mathcal{D}, \quad (58)$$

where $e^{x^*} = x^* - x_N^*$. The result then follows directly from Proposition 3.

As pointed out previously, there is a freedom of choice on how to define the inner product and associated norm on X . In fact, one can choose the norm on X so as to minimize the effectivity of the error bound $\Delta_N^{J,\text{BNB}}(\mu)$. We will comment on this issue in Section 5.

4.4 Computational procedure

To evaluate the control and cost functional error bounds $\Delta_N^{u,\text{PER}}(\mu)$, $\Delta_N^{u,\text{ALT}}(\mu)$, $\Delta_N^{J,\text{PER}}(\mu)$, and $\Delta_N^{J,\text{ALT}}(\mu)$ (see Sections 4.2.1, 4.2.2 and 4.3.1), we need to compute

1. the dual norms of the state, adjoint, and optimality equation residuals, i.e., $\|r_y(\cdot; \mu)\|_{Y'}$, $\|r_p(\cdot; \mu)\|_{Y'}$, and $\|r_u(\cdot; \mu)\|_{U(\mu)'}$; and
2. the lower and upper bounds $\alpha_a^{\text{LB}}(\mu)$, $C_D^{\text{UB}}(\mu)$, and $\gamma_b^{\text{UB}}(\mu)$.

Since $\|r_y(\cdot; \mu)\|_{Y'}$ and $\|r_p(\cdot; \mu)\|_{Y'}$ can be evaluated using the standard offline-online decomposition [32], we only summarize the computational cost in the offline and online stage. For the computation of the dual norm of the state residual we have to solve $n_y = (2Q_a + Q_b)N + Q_f$ Poisson-type problems in the offline stage, and can then evaluate $\|r_y(\cdot; \mu)\|_{Y'}$ in $\mathcal{O}(n_y^2)$ operations in the online stage for any given parameter $\mu \in \mathcal{D}$ (and associated optimal solution x_N^*). Similarly, for the adjoint residual we require $n_p = (2Q_a + 2Q_d)N + Q_d Q_{yd}$ Poisson problem solves offline, and $\mathcal{O}(n_p^2)$ operations online.

Since the evaluation of $\|r_u(\cdot; \mu)\|_{U(\mu)'}$ is not standard, we provide the necessary details here. From

$$r_u(\psi; \mu) = -(\lambda(u_N^* - u_d) - \mathcal{B}^* p_N^*, \psi)_{U(\mu)} = (\tilde{r}_u(\mu), \psi)_{U(\mu)}, \quad (59)$$

it follows that $\tilde{r}_u(\mu) = -\lambda(u_N^* - u_d) + \mathcal{B}^* p_N^*$ is the Riesz-representation of $r_u(\cdot; \mu) \in U(\mu)'$ with respect to the $(\cdot, \cdot)_{U(\mu)}$ energy inner product. Since $\|r_u(\cdot; \mu)\|_{U(\mu)'} = \|\tilde{r}_u(\mu)\|_{U(\mu)}$, we can compute the dual norm of the optimality equation residual by

$$\|r_u(\cdot; \mu)\|_{U(\mu)'}^2 = \|\tilde{r}_u(\mu)\|_{U(\mu)}^2 = \|\lambda(u_N^* - u_d) - \mathcal{B}^* p_N^*\|_{U(\mu)}^2 \quad (60)$$

$$\begin{aligned} &= \lambda^2 (u_N^*, u_N^*)_{U(\mu)} - 2\lambda (u_N^*, u_d)_{U(\mu)} + \lambda^2 (u_d, u_d)_{U(\mu)} \\ &\quad - 2\lambda (u_N^*, \mathcal{B}^* p_N^*)_{U(\mu)} + 2\lambda (u_d, \mathcal{B}^* p_N^*)_{U(\mu)} + (\mathcal{B}^* p_N^*, \mathcal{B}^* p_N^*)_{U(\mu)} \end{aligned} \quad (61)$$

$$\begin{aligned} &= \lambda^2 (\underline{u}_N^*)^T C_N(\mu) \underline{u}_N^* - 2\lambda (\underline{u}_N^*)^T U_{d,N}(\mu) + \lambda^2 U_{d,d}(\mu) \\ &\quad - 2\lambda (\underline{u}_N^*)^T \underline{B}_N^T(\mu) \underline{p}_N^* + 2\lambda \underline{B}_{d,N}^T(\mu) \underline{p}_N^* + (\underline{p}_N^*)^T \underline{B}_N^*(\mu) \underline{p}_N^*. \end{aligned} \quad (62)$$

The matrix $B_N^*(\mu) \in \mathbb{R}^{2N \times 2N}$ and vector $B_{d,N}(\mu) \in \mathbb{R}^{2N}$ are defined by the entries $(B_N^*(\mu))_{ij} = c(\mathcal{B}^* \zeta_j^y, \mathcal{B}^* \zeta_i^y; \mu)$, and $(B_{d,N}(\mu))_i = b(u_d, \zeta_i^y; \mu)$. For the case of parameter-dependent operators $\mathcal{B}^*(\mu)$, we refer to the discussion in [19]. By exploiting the affine parameter dependence of $c(\cdot, \cdot; \mu)$ and $b(\cdot, \cdot; \mu)$, $B_N^*(\mu)$ and $B_{d,N}(\mu)$ can be assembled online in $4Q_c N^2$ and $2Q_b N$ operations, respectively. The total online cost for computing $\|r_u(\cdot; \mu)\|_{U(\mu)^y}$ is $\mathcal{O}((Q_c + Q_b)N^2)$.

For the construction of the coercivity constant lower bound $\alpha_a^{\text{LB}}(\mu)$ various recipes exist [14, 30, 37]. The specific choices for our numerical examples are stated in Section 5. Simple (yet for our examples effective) upper bounds $C_D^{\text{UB}}(\mu)$ and $\gamma_b^{\text{UB}}(\mu)$ can be computed by solving $Q_d + Q_u$ generalized eigenvalue problems in the offline stage and then assembled in $\mathcal{O}(Q_d + Q_u)$ operations online (see [19] for more details). In general (arbitrarily tight) upper bounds can be obtained by applying the successive constraint method.

In summary, the online evaluation of the error bounds $\Delta_N^{u,\text{PER}}(\mu)$, $\Delta_N^{u,\text{ALT}}(\mu)$, $\Delta_N^{J,\text{PER}}(\mu)$, and $\Delta_N^{J,\text{ALT}}(\mu)$ involves an operation count that is *independent* of the dimension of the finite element spaces \mathcal{N}_Y and \mathcal{N}_U .

For the evaluation of the error bounds $\Delta_N^{x,\text{BNB}}(\mu)$, and $\Delta_N^{J,\text{BNB}}(\mu)$ described in Sections 4.2.3 and 4.3.2, we need to compute

1. the dual norm of the saddle point residual $\|r_x(\cdot; \mu)\|_{X'}$; and
2. the constant $\beta_{\text{Ba}}^{\text{LB}}(\mu)$.

The computational procedure and effort to compute $\|r_x(\cdot; \mu)\|_{X'}$ are the same as for evaluating $\|r_y(\cdot; \mu)\|_{Y'}$, $\|r_p(\cdot; \mu)\|_{Y'}$, and $\|r_u(\cdot; \mu)\|_{U(\mu)^y}$. However, computing a lower bound $\beta_{\text{Ba}}^{\text{LB}}(\mu)$ for the stability constant is quite involved and requires a large computational effort in the offline stage [29]. Alternatively, interpolation techniques can be used, but doing so unfortunately sacrifices the rigor of the error bound [28].

5 Numerical results

In this section we present two numerical examples: i) a Graetz flow and ii) a heat transfer problem motivated by hyperthermia cancer treatment. Both problems involve a distributed control over the entire domain. We stress that, throughout this section, we use the actual stability constant $\beta_{\text{Ba}}(\mu)$ and *not* its lower bound $\beta_{\text{Ba}}^{\text{LB}}(\mu)$ for the evaluation of the BNB-bounds (49) and (57). The reason is the high computational cost and implementation effort required to obtain $\beta_{\text{Ba}}^{\text{LB}}(\mu)$ in combination with the fact that the BNB-bounds are just used for comparison here (and are not our original contribution). The computations were done in Matlab on a computer with a 2.6 GHz Intel Core i7 processor and 16 GB of RAM.

5.1 Graetz flow problem

We consider a linear-quadratic optimal control problem governed by a steady Graetz flow in a two-dimensional domain based on the numerical examples in [27, 29]. The spatial domain, given by $\Omega = (0, 2.5) \times (0, 1)$, is subdivided into the three subdomains $\Omega_1 = [0.2, 0.8] \times [0.3, 0.7]$, $\Omega_2 = [1.2, 2.5] \times [0.3, 0.7]$, and $\Omega_3 = \Omega \setminus \{\Omega_1 \cup \Omega_2\}$; see Figure 1a. We impose homogeneous Neumann and non-homogeneous Dirichlet boundary conditions on Γ_N and $\Gamma_D = \Gamma_{D_1} \cup \Gamma_{D_2}$, respectively. The amount of heat supply in the entire domain Ω is regulated

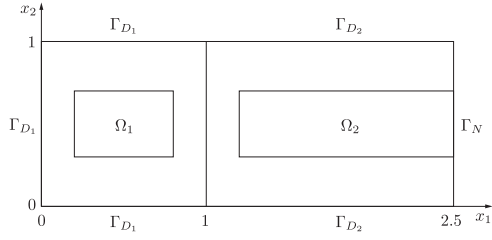


Fig. 1a: Domain Ω for the Graetz flow problem with distributed control.

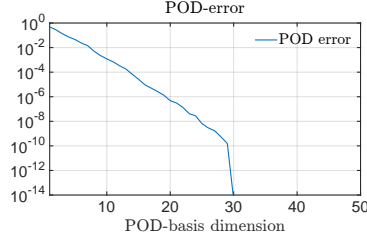


Fig. 1b: POD-error for the control in dependence of the basis dimension.

by the distributed control function $u_e \in U_e := L^2(\Omega)$. The parametrized optimal control problem is then

$$\begin{aligned} \min_{y_e \in Y_e^D, u_e \in U_e} J(y_e, u_e; \mu) &= \frac{1}{2} \|y_e - y_{d,e}(\mu)\|_{L^2(\Omega_1 \cup \Omega_2)}^2 + \frac{\lambda}{2} \|u_e - u_{d,e}\|_{L^2(\Omega)}^2 \\ \text{s.t.} \quad \frac{1}{\mu_1} \int_{\Omega} \nabla y_e \cdot \nabla v \, dx + \int_{\Omega} \beta(x) \cdot \nabla y_e v \, dx &= \int_{\Omega} u_e v \, dx \quad \forall v \in Y_e^D, \end{aligned} \quad (63)$$

for the given parabolic velocity field $\beta(x) = (x_2(1-x_2), 0)^T$ and $Y_e^D = \{v \in H^1(\Omega) : v|_{\Gamma_{D_1}} \equiv 1, v|_{\Gamma_{D_2}} \equiv 2\}$. The parameter μ_1 describes the Péclet number of the flow, and the parametrized desired state is given by $y_{d,e}(\mu) \equiv \mu_2$ on Ω_1 and $y_{d,e}(\mu) \equiv \mu_3$ on Ω_2 . The full parameter domain is $\mathcal{D} = [3, 20] \times [0.5, 1.5] \times [1.5, 2.5]$. For the cost functional we set $u_{d,e} \equiv 0$. In Section 5.3 we consider different values for the regularization parameter λ . However, for the remainder of this subsection we will keep the regularization parameter $\lambda = 0.01$ fixed. We choose the inner product $(w, v)_{Y_e} = \frac{1}{\mu_1^{\text{ref}}} \int_{\Omega} \nabla w \cdot \nabla v \, dx + \frac{1}{2} \left(\int_{\Omega} \beta(x) \cdot \nabla w v \, dx + \int_{\Omega} \beta(x) \cdot \nabla v w \, dx \right)$ for $\mu_1^{\text{ref}} = 3$; we may hence choose $\alpha_a^{\text{LB}}(\mu) = \min(\mu_1^{\text{ref}}/\mu_1, 1)$ in (11). For the control space U_e we use the usual L^2 -norm and inner product. After introducing suitable lifting functions that take into account the non-homogeneous Dirichlet boundary conditions, we can reformulate the problem in terms of the space $Y_e = \{v \in H^1(\Omega) : v|_{\Gamma_{D_1} \cup \Gamma_{D_2}} \equiv 0\}$; the considered problem then satisfies the affine representation (4) of all involved quantities with $Q_a = 2$, $Q_b = Q_d = Q_c = 1$, $Q_f = 2$, and $Q_{yd} = 3$ (taking into account the affine terms required for the lifting functions). For details regarding the involved bilinear forms and functionals, the lifting procedure, and the construction of $\alpha_a^{\text{LB}}(\mu)$ we refer to [19, 27, 29].

For the truth discretization we consider linear finite element approximation spaces $Y \subset Y_e$ and $U \subset U_e$ for the state, adjoint, and control variables. The number of degrees of freedom is $\dim(Y) = \mathcal{N}_Y = 10,801$ and $\dim(U) = \mathcal{N}_U = 11,148$; hence the total dimension of the truth optimality system is $2\mathcal{N}_Y + \mathcal{N}_U = 32,750$.

We construct the reduced basis spaces $Y_N \subset Y$ and $U_N \subset U$ according to the greedy sampling procedure described in Section 3.2. To this end, we employ the train sample $\Xi_{\text{train}} \subset \mathcal{D}$ consisting of $n_{\text{train}} = 10 \cdot 7 \cdot 7 = 490$ equidistant parameter points over \mathcal{D} . We sample on the relative ALT control error bound $\Delta_N^{u, \text{ALT}}(\mu) / \|u_N^*(\mu)\|_{U(\mu)}$. The desired error tolerance is $\varepsilon_{\text{tol}, \text{min}} = 10^{-4}$, and the initial parameter value is $\mu^1 = (3, 0.5, 1.5)^T$. We also introduce a parameter test sample $\Xi_{\text{test}} \subset \mathcal{D}$ of size $n_{\text{test}} = 20$ with a uniform-random distribution in \mathcal{D} .

On the product space $X = Y \times U \times Y$, we define for $\vartheta_1 = (\varphi_1, \psi_1, \phi_1) \in X$ and $\vartheta_2 = (\varphi_2, \psi_2, \phi_2) \in X$ the energy inner product as $(\vartheta_1, \vartheta_2)_{X(\mu)} = (\varphi_1, \varphi_2)_Y + (\psi_1, \psi_2)_{U(\mu)} + (\phi_1, \phi_2)_Y$, and associated energy norm as $\|\vartheta\|_{X(\mu)} = (\vartheta, \vartheta)_{X(\mu)}^{1/2} = (\|\varphi\|_Y^2 + \|\psi\|_{U(\mu)}^2 + \|\phi\|_Y^2)^{1/2}$. In

Section 5.3 we will also consider a scaled energy inner product and norm given by $(\vartheta_1, \vartheta_2)_{X_\lambda(\mu)} = (\varphi_1, \varphi_2)_Y + \lambda(\psi_1, \psi_2)_{U(\mu)} + (\phi_1, \phi_2)_Y$ and $\|\vartheta\|_{X_\lambda(\mu)} = (\vartheta, \vartheta)_{X_\lambda(\mu)}^{1/2} = (\|\varphi\|_Y^2 + \lambda\|\psi\|_{U(\mu)}^2 + \|\phi\|_Y^2)^{1/2}$. This corresponds to $C_{U,X} = 1$ respectively $C_{U,X} = \sqrt{\lambda}$ in the remark after Proposition 3. We recall that the PER- and ALT-bounds measure the error in the energy control norm $\|\cdot\|_{U(\mu)}$, which is the more relevant norm for geometry parametrizations. Since for the Graetz flow problem we do not consider any geometrical parametrization, the reference and energy control norms coincide. Also, in the heat transfer problem of Section 5.2 — involving a parametrized domain — we do not observe any remarkable differences between the results for the reference and energy norms (i.e., the norm equivalence constants are close to one). For this reason, we focus on the results based on the energy norm.

In Figure 1b we present the POD-error decay of the control-snapshots over $\mathcal{E}_{\text{train}}$.⁶ The error-decay indicates how many snapshots we need to approximate the control for a desired accuracy: Any optimal control in the training set can be represented by roughly 14 POD basis functions to a precision of $1\text{E-}4$. Although POD is only optimal in the L^2 -sense over the training set, it serves as a good indicator of the error expected from our reduced basis approach (see Section 8.1.4 in [32]). Indeed, with 16 control basis functions the reduced basis approximation exhibits a relative L^∞ -error of less than $1\text{E-}4$. With only three more basis functions ($N = 19$) this accuracy can even be guaranteed *a posteriori* using the ALT-bound (see Table 1).

Table 1: Control variable in Graetz flow example: error convergence, error bounds, and effectivities as a function of N .

N	$\varepsilon_{N,\text{max,rel}}^u$	$\Delta_{N,\text{max,rel}}^{u,\text{BNB}}$	$\bar{\eta}_N^{u,\text{BNB}}$	$\Delta_{N,\text{max,rel}}^{u,\text{PER}}$	$\bar{\eta}_N^{u,\text{PER}}$	$\Delta_{N,\text{max,rel}}^{u,\text{ALT}}$	$\bar{\eta}_N^{u,\text{ALT}}$
2	1.12 E+00	1.76 E+02	1.35 E+02	1.12 E+02	4.68 E+01	4.01 E+01	1.49 E+01
4	4.96 E-01	9.18 E+01	9.58 E+01	7.84 E+00	2.66 E+01	1.72 E+00	4.34 E+00
8	3.07 E-02	3.82 E+00	7.82 E+01	4.58 E-01	2.25 E+01	1.43 E-01	6.27 E+00
12	1.66 E-03	1.36 E-01	6.89 E+01	4.03 E-02	1.51 E+01	7.74 E-03	4.49 E+00
16	9.67 E-05	8.19 E-03	9.20 E+01	1.95 E-03	2.33 E+01	3.43 E-04	4.95 E+00
19	1.26 E-05	8.13 E-04	7.82 E+01	2.46 E-04	1.49 E+01	4.86 E-05	3.64 E+00

In Table 1 we present, as a function of N , the maximum relative control error $\varepsilon_{N,\text{max,rel}}^u$ and the maximum relative error bounds $\Delta_{N,\text{max,rel}}^{u,\text{BNB}}$, $\Delta_{N,\text{max,rel}}^{u,\text{PER}}$, $\Delta_{N,\text{max,rel}}^{u,\text{ALT}}$, as well as the corresponding mean effectivities $\bar{\eta}_N^{u,\text{BNB}}$, $\bar{\eta}_N^{u,\text{PER}}$, $\bar{\eta}_N^{u,\text{ALT}}$. Here, $\varepsilon_{N,\text{max,rel}}^u$ is the maximum over $\mathcal{E}_{\text{test}}$ of $\|e^{u^*}(\mu)\|_{U(\mu)} / \|u^*(\mu)\|_{U(\mu)}$, $\Delta_{N,\text{max,rel}}^{u,\bullet}$ is the maximum over $\mathcal{E}_{\text{test}}$ of $\Delta_N^{u,\bullet}(\mu) / \|u^*(\mu)\|_{U(\mu)}$, and $\bar{\eta}_N^{u,\bullet}$ is the average over $\mathcal{E}_{\text{test}}$ of $\Delta_N^{u,\bullet}(\mu) / \|e^{u^*}(\mu)\|_{U(\mu)}$. We observe that the control error and all three error bounds are decreasing rapidly with increasing reduced basis dimension N . The greedy sampling procedure guarantees the prescribed sampling tolerance $\varepsilon_{\text{tol,min}} = 10^{-4}$ for the normalized error bound $\Delta_N^{u,\text{ALT}}(\mu) / \|u^*(\mu)\|_{U(\mu)}$ over the training set $\mathcal{E}_{\text{train}}$ after selecting only $N_{\text{max}} = 19$ parameter snapshots. We note that the effectivities of the BNB-bound

⁶ The error for a POD basis of size N_{POD} is given by $(\sum_{i=N_{\text{POD}}+1}^{n_{\text{train}}} \sigma_i^2)^{1/2}$, where σ_i , $1 \leq i \leq n_{\text{train}}$, are the singular values (in decreasing order) of $\frac{1}{\sqrt{n_{\text{train}}}} \mathbb{U}^{1/2} S$. Here, \mathbb{U} is the finite element matrix associated with the reference inner product $(\cdot, \cdot)_U = (\cdot, \cdot)_{U(\mu^{\text{ref}})}$, and $S \in \mathbb{R}^{\mathcal{N}_U \times n_{\text{train}}}$ is the snapshot matrix of optimal controls $u^*(\mu)$ for all $\mu \in \mathcal{E}_{\text{train}}$. See also [31].

are slightly larger than the ones of the PER-bound, and that both are significantly larger than the ones of the ALT-bound. The ALT-bound clearly performs best with effectivities close to one for all values of N (except for $N = 2$). Again, the BNB-bound is computed with $\beta_{\text{Ba}}(\mu)$ instead of $\beta_{\text{Ba}}^{\text{LB}}(\mu)$, and the effectivities may thus be considerably larger in actual practice.

Table 2: Combined variable x in Graetz flow example: error convergence, error bounds, and effectivities as a function of N .

N	$\varepsilon_{N,\max,\text{rel}}^x$	$\Delta_{N,\max,\text{rel}}^{x,\text{BNB}}$	$\bar{\eta}_N^{x,\text{BNB}}$	$\Delta_{N,\max,\text{rel}}^{x,\text{PER}}$	$\bar{\eta}_N^{x,\text{PER}}$	$\Delta_{N,\max,\text{rel}}^{x,\text{ALT}}$	$\bar{\eta}_N^{x,\text{ALT}}$
2	7.00 E-02	8.54 E+00	1.02 E+02	7.39 E+00	1.13 E+02	2.67 E+00	3.48 E+01
4	3.15 E-02	3.46 E+00	8.26 E+01	1.05 E+00	7.35 E+01	1.16 E-01	1.08 E+01
8	1.71 E-03	2.03 E-01	7.01 E+01	3.02 E-02	6.54 E+01	8.35 E-03	1.73 E+01
12	6.84 E-05	7.15 E-03	6.26 E+01	2.67 E-03	4.16 E+01	6.06 E-04	1.09 E+01
16	2.87 E-06	4.58 E-04	7.99 E+01	2.83 E-04	6.72 E+01	3.91 E-05	1.24 E+01
19	4.53 E-07	4.55 E-05	6.47 E+01	1.63 E-05	4.01 E+01	3.40 E-06	9.10 E+00

Since the BNB-bound is actually a bound for the combined error $\|e^{x,*}\|_{X(\mu)}$, we also present results for the combined variable x . In Table 2 we compare, as function of N , the maximum relative combined error $\varepsilon_{N,\max,\text{rel}}^x$ and the maximum relative error bounds $\Delta_{N,\max,\text{rel}}^{x,\text{BNB}}$, $\Delta_{N,\max,\text{rel}}^{x,\text{PER}}$, $\Delta_{N,\max,\text{rel}}^{x,\text{ALT}}$, as well as the corresponding mean effectivities $\bar{\eta}_N^{x,\text{BNB}}$, $\bar{\eta}_N^{x,\text{PER}}$, $\bar{\eta}_N^{x,\text{ALT}}$. Here, $\varepsilon_{N,\max,\text{rel}}^x$ is the maximum over Ξ_{test} of $\|e^{x,*}(\mu)\|_{X(\mu)}/\|x^*(\mu)\|_{X(\mu)}$, $\Delta_{N,\max,\text{rel}}^{x,\bullet}$ is the maximum over Ξ_{test} of $\Delta_N^{x,\bullet}(\mu)/\|x^*(\mu)\|_{X(\mu)}$, and $\bar{\eta}_N^{x,\bullet}$ is the average over Ξ_{test} of $\Delta_N^{x,\bullet}(\mu)/\|e^{x,*}\|_{X(\mu)}$. Note that we obtain this bound for the PER- and ALT-approach by simply combining the control error bound with the state and adjoint optimality error bounds defined in Lemma 3 and 4, respectively. Similar to the results for the control variable, the combined error and all three bounds are decreasing rapidly with increasing reduced basis dimension N . Although the BNB-bound is specifically designed to measure the combined error in the X -norm, its effectivities are comparable to the PER-bound and significantly (almost one order of magnitude) larger than for the ALT-bound.

Table 3: Cost functional J in Graetz flow example: error convergence, error bounds, and effectivities as a function of N .

N	$\varepsilon_{N,\max,\text{rel}}^J$	$\Delta_{N,\max,\text{rel}}^{J,\text{BNB}}$	$\bar{\eta}_N^{J,\text{BNB}}$	$\Delta_{N,\max,\text{rel}}^{J,\text{PER}}$	$\bar{\eta}_N^{J,\text{PER}}$	$\Delta_{N,\max,\text{rel}}^{J,\text{ALT}}$	$\bar{\eta}_N^{J,\text{ALT}}$
2	1.10 E+01	3.38 E+03	2.29 E+03	9.30 E+03	7.12 E+02	3.37 E+03	1.81 E+02
4	1.31 E-01	9.23 E+02	4.51 E+03	4.78 E+01	1.18 E+03	6.25 E+00	1.74 E+02
8	4.90 E-04	1.98 E+00	5.49 E+03	1.42 E-01	5.94 E+02	4.60 E-02	1.72 E+02
12	2.53 E-06	2.59 E-03	3.40 E+03	1.21 E-03	3.60 E+02	2.29 E-04	1.16 E+02
16	1.54 E-09	8.86 E-06	9.32 E+03	2.91 E-06	1.25 E+04	3.91 E-07	1.91 E+03
19	1.21 E-10	8.72 E-08	4.61 E+03	4.53 E-08	5.04 E+02	9.08 E-09	1.08 E+02

Finally, we state in Table 3, as a function of N , the maximum relative cost functional error $\varepsilon_{N,\max,\text{rel}}^J$ and the maximum relative error bounds $\Delta_{N,\max,\text{rel}}^{J,\text{BNB}}$, $\Delta_{N,\max,\text{rel}}^{J,\text{PER}}$, $\Delta_{N,\max,\text{rel}}^{J,\text{ALT}}$, as well as the corresponding mean effectivities $\bar{\eta}_N^{J,\text{BNB}}$, $\bar{\eta}_N^{J,\text{PER}}$, $\bar{\eta}_N^{J,\text{ALT}}$. Here, $\varepsilon_{N,\max,\text{rel}}^J$ is the

maximum over Ξ_{test} of $|J^*(\mu) - J_N^*(\mu)|/J^*(\mu)$, $\Delta_{N,\text{max,rel}}^{J,\bullet}$ is the maximum over Ξ_{test} of $\Delta_N^{J,\bullet}(\mu)/J^*(\mu)$, and $\bar{\eta}_N^{J,\bullet}$ is the average over Ξ_{test} of $\Delta_N^{J,\bullet}(\mu)/|J^*(\mu) - J_N^*(\mu)|$. Again, a rapid decrease of the error and error bounds can be observed. The BNB- and PER-bound effectivities have the same order of magnitude whereas the ALT-bound again performs considerably better. We note that the (generally) large effectivities for the cost are clearly not desirable, but not particularly deleterious in the reduced basis context given the rapid convergence: the additional number of required basis functions due to the overestimation is only logarithmic in the effectivity for the observed exponential convergence with N .

We finally consider the online computational cost for solving the reduced basis optimal control problem compared to the truth optimal control problem. On average (over Ξ_{test}) it takes 0.49 seconds to solve the truth optimal control problem based on our finite element discretization. Depending on the reduced basis dimension $1 \leq N \leq N_{\text{max}} = 19$ it takes between 1.19 and 2.01 milliseconds to solve the reduced basis optimal control problem (without error bounds); this results in speed-ups ranging from 244 to 412. Taking into account the computation of the error bounds (consisting mainly of the online residual calculation and evaluation of $\alpha_a^{\text{LB}}(\mu)$) the online cost for the reduced basis solution ranges from 1.61 to 2.11 milliseconds, which in turn corresponds to a speed-up of 232 up to 304. Note that the computational time required for the error bound computation is only a small fraction of the reduced basis solution time.

5.2 Heat transfer problem

Next we consider a linear-quadratic optimal control problem governed by steady heat conduction in a parametrized two-dimensional domain. The spatial domain is given by $\Omega^o = (0, 5) \times (0, 5)$ and is subdivided into the three subdomains $\Omega_1^o(\mu) = \Omega^o \setminus \{\Omega_2^o \cup \Omega_3^o(\mu)\}$, $\Omega_2^o = \{(1, 4) \times (1, 2)\} \cup \{(1, 2) \times (1, 4)\}$, and $\Omega_3^o(\mu) = (\mu_1 - 0.5, \mu_1 + 0.5) \times (\mu_2 - 0.5, \mu_2 + 0.5)$.⁷ Here, the parameter $\mu = (\mu_1, \mu_2)^T \in \mathcal{D} = [3, 4] \times [3, 4]$ describes the horizontal and vertical translation of the square $\Omega_3^o(\mu)$ in the upper right corner of the domain Ω^o . A sketch of the domain is shown in Figure 2a. The temperature satisfies Laplace's equation in Ω^o with

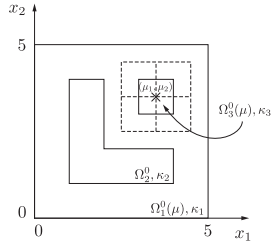


Fig. 2a: Parametrized domain $\Omega^o(\mu)$ for the heat transfer problem with distributed control.

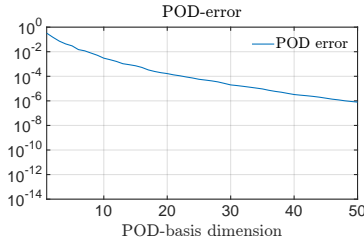


Fig. 2b: POD-error for the control in dependence of the basis dimension.

continuity of temperature and heat flux across subdomain interfaces. The (reference) conductivity in the subdomain $\Omega_1^o(\mu)$ is set to unity, whereas the normalized conductivity is

⁷ The superscript “o” indicates quantities related to the original parameter-dependent domain $\Omega^o(\mu)$, whereas no superscript refers to the parameter-independent reference domain $\Omega = \Omega^o(\mu^{\text{ref}})$.

$\kappa_2 = 0.2$ in the subdomain Ω_2^o and $\kappa_3 = 5$ in the subdomain $\Omega_3^o(\mu)$. We impose zero Dirichlet conditions on the whole domain boundary Γ^o . The amount of heat supply in the entire domain Ω^o is regulated by the distributed control function $u_e^o \in U_e^o := L^2(\Omega^o)$.

The parametrized optimal control problem then reads

$$\begin{aligned} \min_{y_e^o \in Y_e^o, u_e^o \in U_e^o} J(y_e^o, u_e^o; \mu) &= \frac{1}{2} \|y_e^o - y_{d,e}^o\|_{L^2(\Omega_2^o \cup \Omega_3^o(\mu))}^2 + \frac{\lambda}{2} \|u_e^o - u_{d,e}^o\|_{L^2(\Omega^o)}^2 \\ \text{s.t. } \sum_{i=1}^3 \kappa_i \int_{\Omega_i^o(\mu)} \nabla y_e^o \cdot \nabla v \, dx &= \int_{\Omega^o} u_e^o v \, dx \quad \forall v \in Y_e^o = H_0^1(\Omega^o). \end{aligned} \quad (64)$$

The desired state is given by $y_{d,e}^o \equiv 1$ in Ω_2^o and $y_{d,e}^o \equiv 0$ in $\Omega_3^o(\mu)$, and the desired control is $u_{d,e}^o \equiv 0$. As for the Graetz flow example we will keep the regularization parameter $\lambda = 0.01$ fixed for the remainder of this subsection. In Section 5.3 we consider different values for the regularization parameter λ . After recasting the problem to a reference domain Ω with corresponding subdomains $\Omega_{1,3} = \Omega_{1,3}^o(\mu^{\text{ref}})$ for $\mu^{\text{ref}} = (3.5, 3.5)^T$ [32], we can reformulate the problem in terms of the spaces $Y_e = H_0^1(\Omega)$ and $U_e = L^2(\Omega)$. We also obtain the affine representations (4) of all involved quantities with $Q_a = 15$, $Q_b = Q_c = 4$, $Q_d = 1$, $Q_f = 0$, and $Q_{yd} = 1$; see [19] for details.

The problem is motivated by hyperthermia treatment of cancer, where the subdomain Ω_2^o could be interpreted as tumor tissue and the subdomain $\Omega_3^o(\mu)$ as so-called risk tissue. Hence, the goal is to heat up only the damaged part of the body ($y_{d,e}^o \equiv 1$ in Ω_2^o) but not the regions at risk ($y_{d,e}^o \equiv 0$ in $\Omega_3^o(\mu)$). Furthermore, the approach presented here has also been applied to a radiation treatment planning problem [1].

We choose the inner product $(w, v)_{Y_e} = \sum_{i=1}^3 \kappa_i \int_{\Omega_i} \nabla w \cdot \nabla v \, dx$. To compute a lower bound $\alpha_a^{\text{LB}}(\mu)$ for the coercivity constant in (11), we use the successive constraint method (SCM) [14, 6], where we chose the following parameters: $J^{\text{SCM}} = 35 \cdot 35 = 1225$ equidistant training points over \mathcal{D} , $M^{\text{SCM}} = 2$ coercivity and $M_+^{\text{SCM}} = 4$ positivity constraints. A required tolerance of $\varepsilon^{\text{SCM}} = 0.2$ then selects $K^{\text{SCM}} = 53$ parameters in the SCM offline phase. The (reference) inner product for the control space U_e is given by $(\cdot, \cdot)_U = c(\cdot, \cdot, \mu^{\text{ref}})$.

We next introduce linear truth finite element approximation spaces $Y \subset Y_e = H_0^1(\Omega)$ and $U \subset U_e = L^2(\Omega)$ for the state, adjoint, and control variables. The number of degrees of freedom is $\dim(Y) = \mathcal{N}_Y = 18,117$ and $\dim(U) = \mathcal{N}_U = 18,517$; hence the dimension of the truth optimality system is $2\mathcal{N}_Y + \mathcal{N}_U = 54,751$.

We present results for the solution of the truth optimal control problem (64) for different parameter values in Figure 3. We plot the optimal temperature distribution and optimal control, and state the associated cost functional value. We note that all parameters have a strong influence on the solution of the optimal control problem: the temperature, optimal control, and optimal cost functional value vary significantly.

Again, we construct the reduced basis spaces $Y_N \subset Y$ and $U_N \subset U$ according to the greedy sampling procedure described in Section 3.2. The training set $\mathcal{E}_{\text{train}} \subset \mathcal{D}$ consists of $n_{\text{train}} = 15 \cdot 15 = 225$ equidistant parameter points over \mathcal{D} . We sample on the relative ALT control error bound $\Delta_N^{u, \text{ALT}}(\mu) / \|u_N^*(\mu)\|_{U(\mu)}$, set the error tolerance to $\varepsilon_{\text{tol}, \text{min}} = 10^{-4}$, and choose as initial parameter value $\mu^1 = (3, 3)^T$. We obtain $N_{\text{max}} = 45$ to achieve the desired tolerance. The test sample $\mathcal{E}_{\text{test}} \subset \mathcal{D}$ consists of $n_{\text{test}} = 20$ random parameter points distributed uniformly in \mathcal{D} .

To assess the overall quality of our reduced basis approximation, we again present the POD-error decay of the control snapshots over $\mathcal{E}_{\text{train}}$ in Figure 2b. We observe that the error decay is much slower than in the previous example: Although we have one parameter less,

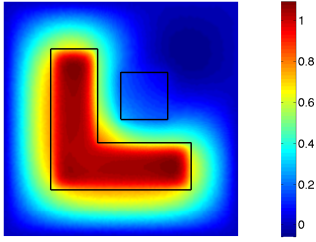


Fig. 3a: Optimal state $y^*(\mu)$,
 $(\mu_1, \mu_2, \lambda) = (3, 3, 0.01)$, $J^*(\mu) = 0.13$

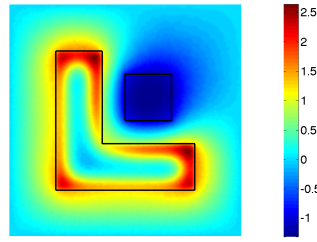


Fig. 3b: Optimal control $u^*(\mu)$,
 $(\mu_1, \mu_2, \lambda) = (3, 3, 0.01)$, $J^*(\mu) = 0.13$

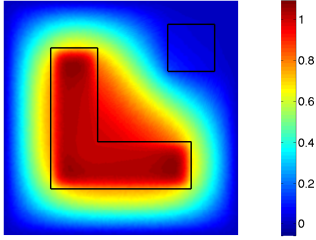


Fig. 3c: Optimal state $y^*(\mu)$,
 $(\mu_1, \mu_2, \lambda) = (4, 4, 0.01)$, $J^*(\mu) = 0.08$

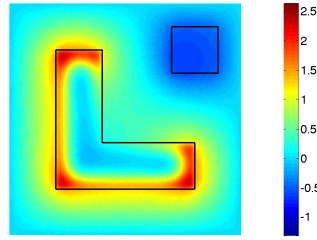


Fig. 3d: Optimal control $u^*(\mu)$,
 $(\mu_1, \mu_2, \lambda) = (4, 4, 0.01)$, $J^*(\mu) = 0.08$

Fig. 3: Optimal state $y^*(\mu)$, optimal control $u^*(\mu)$, and optimal cost functional value $J^*(\mu)$ for different representative parameter values.

the POD now requires roughly 23 basis functions to represent any optimal control in the training set $\mathcal{E}_{\text{train}}$ to a precision of $1 \text{E-}4$. The reduced basis approximation exhibits a similar error decay, i.e., we also require approximately 23 control basis functions to obtain a relative L^∞ -error of less than $1 \text{E-}4$.

Following the presentation of the numerical results for the Graetz flow example in the last section, we present the maximum relative errors and bounds, as well as the average effectivities for the control, the combined variable x , and the cost functional in Tables 4–6. We first observe that the convergence is slower than in the Graetz flow examples due to the higher parametric complexity of this example. Also, the effectivities are consistently higher. For the control variable the effectivities of the BNB-bound and PER-bound are roughly the same, whereas for the combined variable and the cost functional the PER-bound effectivity is approximately one order of magnitude higher than the one of the BNB-bound. Taking into account the additional overestimation if $\beta_{\text{Ba}}^{\text{LB}}(\mu)$ is used instead of $\beta_{\text{Ba}}(\mu)$, the performance of the BNB-bound and PER-bound would likely be equivalent in practice. For all three quantities, however, the ALT-bound again performs best: the overestimation is considerably lower than with the other two approaches.

We finally consider the online computational cost for solving the reduced basis optimal control problem in comparison with the truth optimal control problem. On average (over $\mathcal{E}_{\text{test}}$) it takes 1.23 seconds to solve the truth optimal control problem based on our finite element discretization. Depending on the reduced basis dimension $1 \leq N \leq N_{\text{max}} = 45$, it takes between 1.43 and 5.91 milliseconds to solve the reduced basis optimal control problem resulting in speed-ups ranging from 208 to 860. Taking into account the computation of the

Table 4: Control variable in heat transfer example: error convergence, error bounds, and effectivities as a function of N .

N	$\epsilon_{N,\max,\text{rel}}^u$	$\Delta_{N,\max,\text{rel}}^{u,\text{BNB}}$	$\bar{\eta}_N^{u,\text{BNB}}$	$\Delta_{N,\max,\text{rel}}^{u,\text{PER}}$	$\bar{\eta}_N^{u,\text{PER}}$	$\Delta_{N,\max,\text{rel}}^{u,\text{ALT}}$	$\bar{\eta}_N^{u,\text{ALT}}$
2	1.01 E-01	1.28 E+02	6.19 E+02	1.66 E+02	7.30 E+02	3.71 E+00	2.16 E+01
8	7.16 E-03	3.54 E+00	4.25 E+02	3.86 E+00	4.71 E+02	1.18 E-01	1.56 E+01
16	1.21 E-03	3.09 E-01	4.65 E+02	3.04 E-01	5.33 E+02	1.32 E-02	1.86 E+01
24	8.40 E-05	4.77 E-02	4.89 E+02	5.37 E-02	5.56 E+02	1.71 E-03	2.09 E+01
32	2.22 E-05	1.02 E-02	5.49 E+02	1.72 E-02	6.37 E+02	4.72 E-04	2.39 E+01
40	1.09 E-05	4.38 E-03	6.08 E+02	4.43 E-03	6.91 E+02	1.93 E-04	2.54 E+01
45	1.52 E-06	1.44 E-03	7.52 E+02	1.52 E-03	8.55 E+02	4.21 E-05	2.96 E+01

Table 5: Combined variable x in heat transfer example: error convergence, error bounds, and effectivities as a function of N .

N	$\epsilon_{N,\max,\text{rel}}^x$	$\Delta_{N,\max,\text{rel}}^{x,\text{BNB}}$	$\bar{\eta}_N^{x,\text{BNB}}$	$\Delta_{N,\max,\text{rel}}^{x,\text{PER}}$	$\bar{\eta}_N^{x,\text{PER}}$	$\Delta_{N,\max,\text{rel}}^{x,\text{ALT}}$	$\bar{\eta}_N^{x,\text{ALT}}$
2	1.19 E-01	1.02 E+02	4.55 E+02	1.68 E+03	4.95 E+03	3.82 E+01	1.40 E+02
8	6.58 E-03	2.85 E+00	3.43 E+02	2.91 E+01	3.41 E+03	8.61 E-01	1.10 E+02
16	1.11 E-03	2.49 E-01	3.63 E+02	2.56 E+00	3.78 E+03	6.95 E-02	1.28 E+02
24	8.75 E-05	3.71 E-02	3.83 E+02	4.93 E-01	3.89 E+03	1.60 E-02	1.41 E+02
32	2.40 E-05	8.15 E-03	4.04 E+02	1.81 E-01	4.16 E+03	5.03 E-03	1.51 E+02
40	1.13 E-05	3.47 E-03	4.26 E+02	2.52 E-02	4.25 E+03	8.56 E-04	1.52 E+02
45	2.36 E-06	1.17 E-03	4.60 E+02	1.22 E-02	4.62 E+03	3.48 E-04	1.60 E+02

Table 6: Cost functional J in heat transfer example: error convergence, error bounds, and effectivities as a function of N .

N	$\epsilon_{N,\max,\text{rel}}^J$	$\Delta_{N,\max,\text{rel}}^{J,\text{BNB}}$	$\bar{\eta}_N^{J,\text{BNB}}$	$\Delta_{N,\max,\text{rel}}^{J,\text{PER}}$	$\bar{\eta}_N^{J,\text{PER}}$	$\Delta_{N,\max,\text{rel}}^{J,\text{ALT}}$	$\bar{\eta}_N^{J,\text{ALT}}$
2	3.48 E-02	1.12 E+03	1.59 E+04	1.77 E+04	1.71 E+05	4.04 E+02	4.69 E+03
8	6.67 E-05	1.09 E+00	2.68 E+04	9.46 E+00	3.18 E+05	2.85 E-01	8.22 E+03
16	1.09 E-06	1.30 E-02	3.01 E+04	5.79 E-02	3.79 E+05	2.60 E-03	1.24 E+04
24	1.07 E-08	2.04 E-04	2.39 E+04	1.95 E-03	3.29 E+05	6.34 E-05	1.05 E+04
32	1.83 E-09	1.26 E-05	1.75 E+04	1.91 E-04	2.07 E+05	5.32 E-06	7.02 E+03
40	3.17 E-10	2.54 E-06	1.41 E+04	1.23 E-05	1.56 E+05	4.98 E-07	5.33 E+03
45	1.40 E-11	2.27 E-07	2.44 E+04	1.43 E-06	3.96 E+05	4.11 E-08	1.29 E+04

error bounds (consisting mainly of the online residual calculation and evaluation of $\alpha_a^{\text{LB}}(\mu)$) the online cost for the reduced basis solution ranges from 2.21 to 9.02 milliseconds, which in turn corresponds to a speed-up of 136 up to 557. Although the fraction of the total time required for the error bound computation is now higher than for the Graetz example, the error bound computation still takes less time than solving the reduced basis optimal control problem.

5.3 Performance of error bounds for varying regularization parameter

In this section we investigate the behavior of the parametrized optimal control problem and the performance of the error bounds for different choices of λ . We again consider the Graetz flow and heat transfer problem introduced in the last two sections, and generate five different reduced basis spaces for $\lambda = 1, 10^{-1}, 10^{-2}, 10^{-3},$ and 10^{-4} using the greedy sampling procedure. In Table 7, we present for each λ the number of reduced basis functions N_{\max} required to achieve the prescribed sampling tolerance $\varepsilon_{\text{tol},\min} = 10^{-4}$ (note that $\lambda = 0.01$ corresponds to the case discussed in the last two sections). As expected, the reduced basis dimension N_{\max} increases for decreasing λ . The main reason for this behavior is the increased parametric complexity for smaller values of λ , although we will next observe that the effectivities of the error bounds (in the greedy sampling we use the relative ALT control error bound) will also increase slightly for decreasing λ .

Table 7: Number of Greedy iterations N_{\max} required to achieve the desired accuracy $\varepsilon_{\text{tol},\min} = 10^{-4}$.

λ		1	10^{-1}	10^{-2}	10^{-3}	10^{-4}
Graetz flow	N_{\max}	13	16	19	22	24
Heat transfer	N_{\max}	35	39	45	50	61

We will now turn to the influence of λ on the error bounds. In Figure 4, we present the average (over the test set Ξ_{test} and reduced basis dimension N) control error bound effectivities, $\Delta_N^{u,\bullet}(\mu)/\|e^{u,\bullet}(\mu)\|_{U(\mu)}$, as a function of λ for the Graetz flow and heat transfer problem. Note that this corresponds to five separate evaluations each for a fixed $\lambda \in \{1, 10^{-1}, 10^{-2}, 10^{-3}, 10^{-4}\}$. In addition to the previous tables we also show two more bounds: the original perturbation bound (denoted by TV) as defined in (17), and the λ -scaled bound BNB- λ , which measures the error in the $\|\cdot\|_{X_\lambda(\mu)}$ -norm instead of the $\|\cdot\|_{X(\mu)}$ -norm. Also recall that the original perturbation bound (17) is not online-efficient, since it requires a state and adjoint truth solve. We first observe that the effectivities of all bounds increase with decreasing λ . Furthermore, they scale — except for the ALT-bound — with approximately $1/\lambda$ for $\lambda \leq 10^{-2}$, whereas the ALT-bound shows approximately a scaling with $1/\sqrt{\lambda}$. We recall our discussion after Proposition 2 explaining this effect. We also observe that the PER-bound performs slightly better than the BNB- λ and BNB-bounds (again, taking the additional overestimation due to $\beta_{\text{Ba}}^{\text{LB}}(\mu)$ into account); however, all three bounds become meaningless for small values of λ . In contrast, the ALT-bound effectivity remains acceptable even for $\lambda = 10^{-4}$ and is remarkably even smaller than the original (online-expensive) perturbation bound for small values of λ .

In Figure 5 and Figure 6, we present the corresponding results for the average combined error bound effectivities, $\Delta_N^{x,\bullet}(\mu)/\|e^{x,\bullet}(\mu)\|_{X(\mu)}$, and average cost functional error bound effectivities, $\Delta_N^{J,\bullet}(\mu)/|J^*(\mu) - J_N^*(\mu)|$, respectively. Note that for the bound BNB- λ , the error is measured in the $X_\lambda(\mu)$ -norm. Overall, we observe a similar behavior as for the control variable. We do note, however, that the effectivity of the λ -scaled bound BNB- λ is in most cases approximately one order of magnitude smaller than for the non-scaled BNB-bound. The scaling thus allows to improve the effectivity especially for the cost functional error bound. Finally, we like to point out that the ratio of maximum and mean effectivities

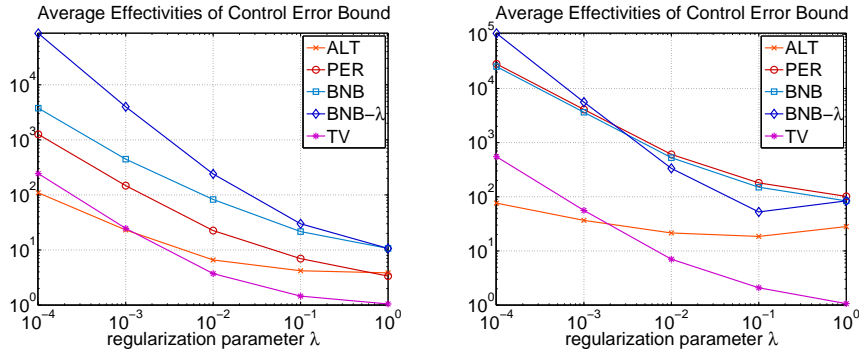


Fig. 4: Control error bound: average effectivities (over N and $\bar{\mathcal{E}}_{\text{test}}$) vs. regularization parameter λ for Graetz flow (left) and heat transfer problem (right).

is always smaller than 20 for all error bounds. This is also true for the examples presented in Section 5.1 and 5.2.

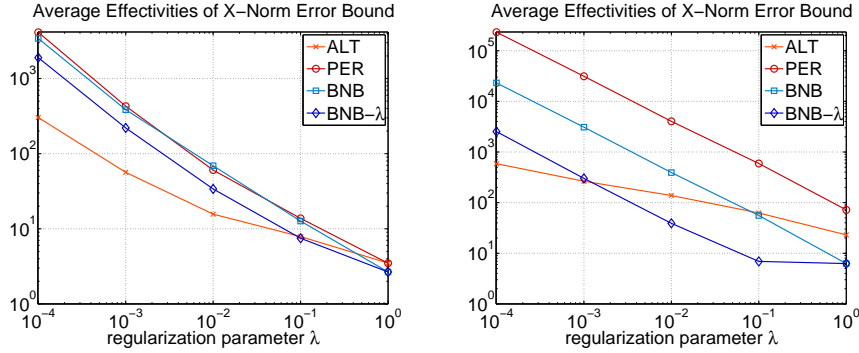


Fig. 5: X -norm error bound: average effectivities (over N and $\bar{\mathcal{E}}_{\text{test}}$) vs. regularization parameter λ for Graetz flow (left) and heat transfer problem (right).

6 Conclusions

The solution of distributed optimal control problems governed by parametrized elliptic PDEs is a challenging and often time-consuming task, especially if one is interested in solutions at many different parameter values. We therefore employed the surrogate model approach and replaced the original high-dimensional PDE approximation by its reduced basis approximation. We also presented two new rigorous *a posteriori* error bounds for the optimal control and associated cost functional. The first one is based on a perturbation argument and is an extension of our previous work in [11, 21] to distributed optimal control problems. The second one is derived directly from the error residual equation of the optimality system and has — to the best of our knowledge — never been proposed before. We showed that

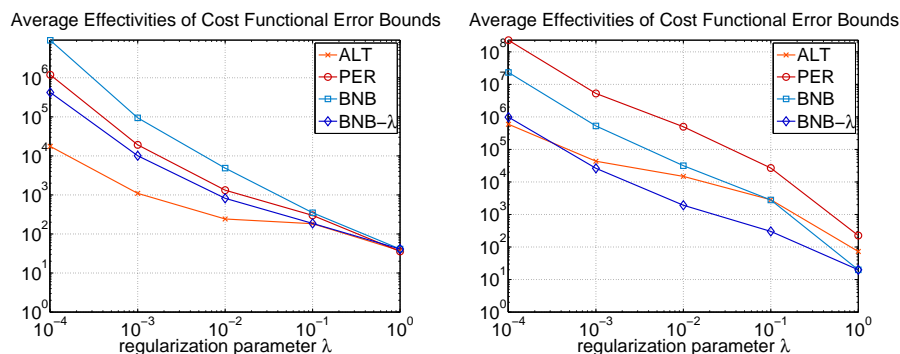


Fig. 6: Cost functional error bound: average effectivities (over N and Ξ_{test}) vs. regularization parameter λ for Graetz flow (left) and heat transfer problem (right).

the reduced basis optimal control problem and the *a posteriori* error bounds can be evaluated efficiently using the standard offline-online computational procedure, resulting in a computational speedup factor of more than 100 in the online stage.

We also compared the two proposed bounds to an *a posteriori* error bound based on the Banach-Nečas-Babuška (BNB) theory proposed in [29]. Concerning the computational cost and implementation effort, the proposed bounds present several advantages compared to the BNB-bound: we only require constants respectively their upper or lower bounds which are inexpensive and straightforward to evaluate, whereas evaluation of a lower bound of the Babuška inf-sup constant for the BNB-bound is (offline-)expensive and difficult to implement. Furthermore, although the performance of the PER-bound is overall similar to the BNB-bound, it has a much wider applicability, e.g., to parabolic problems involving control constraints [20]. The ALT-bound performed best overall, delivering the sharpest *a posteriori* error bounds and the best scaling with respect to the regularization parameter λ . The extension of this bound to parabolic optimal control problems is a topic of current research.

References

1. Ahmedov, B., Grepl, M.A., Herty, M.: Certified reduced order methods for optimal treatment planning. *M3AS: Math. Models Methods Appl. Sci.* **26**(4), 699–727 (2016)
2. Atwell, J.A., King, B.B.: Proper orthogonal decomposition for reduced basis feedback controllers for parabolic equations. *Math. Comput. Model.* **33**(1-3), 1–19 (2001)
3. Becker, R., Kapp, H., Rannacher, R.: Adaptive finite element methods for optimal control of partial differential equations: Basic concept. *SIAM J. Control Optim.* **39**(1), 113–132 (2000)
4. Chen, P., Quarteroni, A.: Weighted reduced basis method for stochastic optimal control problems with elliptic PDE constraint. *SIAM/ASA J. Uncertain. Quantif.* **2**(1), 364–396 (2014)
5. Chen, P., Quarteroni, A., Rozza, G.: Comparison between reduced basis and stochastic collocation methods for elliptic problems. *J. Sci. Comput.* **59**(1), 187–216 (2014)
6. Chen, Y., Hesthaven, J.S., Maday, Y., Rodríguez, J.: Improved successive constraint method based a posteriori error estimate for reduced basis approximation of 2D Maxwell’s problem. *ESAIM: Math. Model. Numer. Anal.* **43**(6), 1099–1116 (2009)
7. Dedè, L.: Reduced basis method and a posteriori error estimation for parametrized linear-quadratic optimal control problems. *SIAM J. Sci. Comput.* **32**(2), 997–1019 (2010)
8. Elman, H.C., Qifeng, L.: Reduced basis collocation methods for partial differential equations with random coefficients. *SIAM/ASA J. Uncertain. Quantif.* **1**(1), 192–217 (2013)
9. Ern, A., Guermond, J.L.: Theory and Practice of Finite Elements, *Applied Mathematical Sciences*, vol. 159. Springer (2010)

10. Gerner, A.L., Veroy, K.: Certified reduced basis methods for parametrized saddle point problems. *SIAM J. Sci. Comput.* **34**(5), A2812–A2836 (2012)
11. Grepl, M.A., Kärcher, M.: Reduced basis a posteriori error bounds for parametrized linear-quadratic elliptic optimal control problems. *C. R. Math.* **349**(15–16), 873–877 (2011)
12. Hager, W.W.: Multiplier methods for nonlinear optimal control. *SIAM J. Numer. Anal.* **27**(4), 1061–1080 (1990)
13. Hinze, M., Pinnau, R., Ulbrich, M., Ulbrich, S.: Optimization with PDE Constraints, *Mathematical Modelling: Theory and Applications*, vol. 23. Springer (2009)
14. Huynh, D.B.P., Rozza, G., Sen, S., Patera, A.T.: A successive constraint linear optimization method for lower bounds of parametric coercivity and inf-sup stability constants. *C. R. Math.* **345**(8), 473–478 (2007)
15. Ito, K., Kunisch, K.: Reduced-order optimal control based on approximate inertial manifolds for nonlinear dynamical systems. *SIAM J. Numer. Anal.* **46**(6), 2867–2891 (2008)
16. Ito, K., Ravindran, S.S.: A reduced basis method for optimal control of unsteady viscous flows. *Int. J. Comput. Fluid D.* **15**, 97–113 (2001)
17. Kammann, E., Tröltzsch, F., Volkwein, S.: A posteriori error estimation for semilinear parabolic optimal control problems with application to model reduction by POD. *ESAIM: Math. Model. Numer. Anal.* **47**(2), 555–581 (2013)
18. Kärcher, M.: The reduced-basis method for parametrized linear-quadratic elliptic optimal control problems. Master's thesis, Technische Universität München (2011)
19. Kärcher, M.: Certified reduced basis methods for parametrized pde-constrained optimization problems. Ph.D. thesis, RWTH Aachen University (submitted)
20. Kärcher, M., Grepl, M.A.: A posteriori error estimation for reduced order solutions of parametrized parabolic optimal control problems. *ESAIM: Math. Model. Numer. Anal.* **48**(6), 1615–1638 (2014)
21. Kärcher, M., Grepl, M.A.: A certified reduced basis method for parametrized elliptic optimal control problems. *ESAIM: Control Optim. Calc. Var.* **20**(2), 416–441 (2014)
22. Kunisch, K., Volkwein, S.: Control of the Burgers equation by a reduced-order approach using proper orthogonal decomposition. *J. Optimiz. Theory App.* **102**, 345–371 (1999)
23. Kunisch, K., Volkwein, S., Xie, L.: HJB-POD based feedback design for the optimal control of evolution problems. *SIAM J. Appl. Dyn. Syst.* **3**, 701–722 (2004)
24. Leugering, G., Engell, S., Griewank, A., Hinze, M., Rannacher, R., Schulz, V., Ulbrich, M., Ulbrich, S. (eds.): *Constrained Optimization and Optimal Control for Partial Differential Equations*. (International Series of Numerical Mathematics). Birkhäuser Basel (2012)
25. Lions, J.L.: *Optimal Control of Systems Governed by Partial Differential Equations*. Springer (1971)
26. Malanowski, K., Büskens, C., Maurer, H.: Convergence of approximations to nonlinear optimal control problems. In: A.V. Fiacco (ed.) *Mathematical Programming with Data Perturbations, Lecture Notes in Pure and Applied Mathematics*, vol. 195, pp. 253–284. Marcel Dekker, Inc. (1997)
27. Negri, F.: Reduced basis method for parametrized optimal control problems governed by PDEs. Master's thesis, Politecnico di Milano (2011)
28. Negri, F., Manzoni, A., Rozza, G.: Reduced basis approximation of parametrized optimal flow control problems for the Stokes equations. *Comput. Math. Appl.* **69**(4), 319–336 (2015)
29. Negri, F., Rozza, G., Manzoni, A., Quarteroni, A.: Reduced basis method for parametrized elliptic optimal control problems. *SIAM J. Sci. Comput.* **35**(5), A2316–A2340 (2013)
30. Prud'homme, C., Rovas, D.V., Veroy, K., Machiels, L., Maday, Y., Patera, A.T., Turinici, G.: Reliable real-time solution of parametrized partial differential equations: Reduced-basis output bound methods. *J. Fluid. Eng.* **124**(1), 70–80 (2002)
31. Quarteroni, A., Manzoni, A., Negri, F.: *Reduced Basis Methods for Partial Differential Equations*. Springer (2015)
32. Rozza, G., Huynh, D.B.P., Patera, A.T.: Reduced basis approximation and a posteriori error estimation for finely parametrized elliptic coercive partial differential equations. *Arch. Comput. Methods Eng.* **15**(3), 229–275 (2008)
33. Rozza, G., Veroy, K.: On the stability of the reduced basis method for Stokes equations in parametrized domains. *Comput. Methods Appl. Mech. Eng.* **196**(7), 1244–1260 (2007)
34. Tröltzsch, F.: *Optimal Control of Partial Differential Equations: Theory, Methods and Applications, Graduate Studies in Mathematics*, vol. 112. American Mathematical Society (2010)
35. Tröltzsch, F., Volkwein, S.: POD a-posteriori error estimates for linear-quadratic optimal control problems. *Comput. Optim. Appl.* **44**(1), 83–115 (2009)
36. Veroy, K., Prud'homme, C., Rovas, D.V., Patera, A.T.: A posteriori error bounds for reduced-basis approximation of parametrized noncoercive and nonlinear elliptic partial differential equations. In: *Proceedings of the 16th AIAA Computational Fluid Dynamics Conference* (2003). AIAA Paper 2003-3847
37. Veroy, K., Rovas, D.V., Patera, A.T.: A posteriori error estimation for reduced-basis approximation of parametrized elliptic coercive partial differential equations: “convex inverse” bound conditioners. *ESAIM: Control Optim. Calc. Var.* **8**, 1007–1028 (2002)